AIAA Paper
No. 74-170

(3)

# THE LONG-TERM PREDICTION OF ARTIFICIAL SATELLITE ORBITS

by
P. J. CEFOLA, A. C. LONG,
and
G. HOLLOWAY, JR.
Computer Sciences Corporation
Silver Spring, Maryland

AIAA PAPER 74-170

AIAA 12th Aerospace Sciences Meeting

WASHINGTON, D.C. / JANUARY 30-FEBRUARY 1, 1974





(33)

# THE LONG-TERM PREDICTION OF ARTIFICIAL SATELLITE ORBITS*

P. J. Cefola,** A. C. Long, and G. Holloway, Jr.
Computer Sciences Corporation
Silver Spring, Maryland

## Abstract

This paper presents a survey of averaging and multirevolution methods. It emphasizes experience with both analytical and numerical averaging. A technical approach with the following features is recommended: (1) averaged variation-of-parameter equations, (2) analytical expressions for oblateness and third-body effects, (3) definite integrals for atmospheric drag and lunar effects (for long period orbits), (4) nonsingular equinoctial element formulation, (5) multistep numerical integration processes, and (6) precise osculating-to-mean element transformation. Several orbital predictions illustrate the contribution of this technical approach to overall accuracy and efficiency. Future development of the analytical averaging method in nonsingular coordinates by automated manipulation of literal series is discussed.

## Introduction

Consider the following applications of orbit prediction methods:

1. Computation of orbital element time histories to support analysis of satellite scientific objectives and engineering constraints (for example, launch window studies)

2. Statistical determination of the mean elements of a satellite orbit at some epoch with an accuracy sufficient to allow meaningful long-term predictions

3. Determination of a gravitational model from very large amounts of satellite or planetary orbiter tracking data

Long-term orbit prediction models are most efficient for these applications where knowledge of the short-period perturbations is not required or where the cost of integrating numerically the precision equations of motion is prohibitively high. Averaging and multirevolution methods for long-term orbit prediction are the subject of this paper. Emphasis is placed on the former.

Averaging methods can be handled either analytically or numerically. The analytical method usually requires a "first order" average of the perturbing potential. The first order qualification indicates that during the averaging process the slowly varying elements are held constant and that the fast variable† (usually the mean anomaly or the mean longitude) varies according to Kepler's laws. The averaged potential is, then, differentiated to obtain the expressions required in the variation-of-parameter (VOP) equations of motion. The resulting closed-form expressions can be used to construct an extremely efficient orbit prediction program. However, the accuracy of the averaged element rates depends on the validity of the various assumptions that are made in deriving the analytical results. A typical set of assumptions is that made in the computation of the averaged third-body potential. The potential is expanded in a power series with the ratio of the distance from central body to satellite to the distance from central body to disturbing body treated as a small parameter. The series is truncated by assuming that higher order terms are negligible. The remaining terms in the expression for the potential are then averaged. To simplify the averaging process, the assumption is made that the disturbing body does not move over one revolution of the satellite. However, such assumptions can limit the applicability of the model for particular orbits.

On the other hand, numerical averaging techniques have the ability to simulate the effect of any small perturbation that can be modeled deterministically. These effects are included by averaging the time derivatives of the orbital elements (including the effects of perturbations) over one or more revolutions of the satellite using a numerical quadrature technique. No mathematical modification to the perturbing acceleration model is required for numerical averaging. However, the right-hand sides of the numerically averaged equations of motion contain definite integrals that are relatively costly in terms of computational requirements. The cost of each derivative evaluation usually is outweighed by the large stepsizes that are possible in the integration of the averaged dynamics.

Multirevolution methods (particularly as developed in References 1, 2, 3, 4, and 5) also attempt to calculate accurately the long-term evolution of the orbit of an artificial satellite about its central body. The fundamental key to this approach is to approximate the derivatives of the mean elements with respect to time by use of a precision integration process. To clarify the

* Work supported under Contract NAS 5-11999 with NASA Goddard Space Flight Center, Greenbelt, Maryland.

** Member, AIAA.

† A fast variable has a nonzero time derivative when the perturbing acceleration is set equal to zero.

issue, compare the VOP precision equation of motion,*

$$\dot{a}_\alpha = \frac{\partial a_\alpha}{\partial \dot{\vec{x}}} \cdot \vec{Q} \tag{1}$$

the multirevolution equation of motion,*

$$\frac{a_\alpha(t+\frac{T}{2}) - a_\alpha(t-\frac{T}{2})}{T} = \frac{1}{T}\int_{t-\frac{T}{2}}^{t+\frac{T}{2}} \frac{\partial a_\alpha}{\partial \dot{\vec{x}}} \cdot \vec{Q}\, dt \tag{2}$$

and the numerically averaged equation of motion,*

$$\dot{\bar{a}}_\alpha = \frac{1}{\bar{T}}\int_{t-\frac{\bar{T}}{2}}^{t+\frac{\bar{T}}{2}} \frac{\partial \bar{a}_\alpha}{\partial \dot{\vec{x}}} \cdot \vec{Q}\, dt \tag{3}$$

In the above equations, the following notation is used,

$a_\alpha$ = precision orbital element

$\dot{a}_\alpha$ = *derivative of* $a_\alpha$ *with respect to time*

$\bar{a}_\alpha$ = mean orbital element

$t$ = time of the derivative evaluation

$T$ = period of the orbit

$\bar{T}$ = mean period of the orbit

$\vec{Q}$ = perturbing acceleration

$\dot{\vec{x}}$ = velocity vector

Clearly, the multirevolution equation of motion [Equation (2)] is an integral form of Equation (1), the high precision equation of motion. In Equation (2), the slowly varying elements, as well as the fast variable, are functions of time. The osculating period represents the time from one reference point to the next. The reference point is usually the nodal crossing[4] or the perifocal passage.[1] The numerically averaged equation of motion [Equation (3)], is a definite integral in which the slowly varying elements are held constant and the fast variable is varied according to Kepler's laws. The $\bar{T}$ in Equation (3) is obtained from the mean semimajor axis, $\bar{a}$, using the relationship

$$\bar{T} = \frac{2\pi}{\bar{n}} = 2\pi\sqrt{\frac{\bar{a}^3}{\mu}} \tag{4}$$

where $\bar{n}$ is the mean Kepler mean motion.

Because the difference $a_\alpha - \bar{a}_\alpha$ is on the order of a small parameter of the problem (for example, $J_2$), the right-hand sides of Equations (2) and (3) are closely related. However, from a computational point of view, there is a significant difference in the cost of evaluating these two expressions. Equation (2) is evaluated using a precision integration process; therefore, a starting procedure must be performed for each evaluation of the long-term rates (assuming that a multistep integration process is used). Also, approximately 100 perturbing acceleration evaluations are typically required in the precision integration of the orbit over one period, T. By comparison, the quadrature process that is used to compute the right-hand side of Equation (3) usually requires no more than 12 (or occasionally 24) perturbing acceleration evaluations over each averaging interval $\bar{T}$. To achieve an efficiency with multirevolution methods that is comparable with that of the averaged orbit generation process, emphasis is placed on developing modified integration formulas to solve the finite difference representation of the equations of motion. These methods require an evaluation of Equation (2) only once every several orbits. The relation of the multirevolution method to Adams' integration is developed in Reference 5.

For long-term predictions where mean element accuracy is required, two limitations of multirevolution methods seem apparent. First, the method is not open to the incorporation of analytical formulas in the same way that analytical averaging can be used in conjunction with numerical averaging. Second, the propagation of the partial derivatives (the state transition matrix) is an open question with regard to multirevolution methods. In contrast, much more work has been done in the propagation of the partial derivatives of the averaged orbital elements (see Reference 6).

The next section of the paper presents a detailed review of the mathematical bases of the various averaging methods. A survey of current averaging computer programs is presented. The following sections consider the formulation of the averaged orbit generation process in nonsingular variables, appropriate numerical integration procedures for the averaged equations of motion, the importance of an osculating-to-mean element transformation, and optimization of the averaged orbit generation process. Numerical examples are presented throughout that illustrate the experience of the authors in these areas. Initial state vectors for the test cases are listed in Tables 1 through 6. Finally, areas are reviewed that are open to further research.

## Averaged Orbit Generation Methods

This section describes the formulation of analytical and numerical averaging methods of orbit computation. Emphasis is placed on specifying the analytical expressions required for an averaging method in a specific set

* For simplicity, equations of motion are presented only for the slowly varying orbital elements. However an analogous relationship exists for the equations of motion of the fast variables.

of coordinates. The relationship of the averaged equations of motion to the precision equations of motion is noted. Recent contributions to the method of averages are cited.

## Mathematical Preliminaries

Averaging methods are based on the precision VOP equations (see Appendix A for derivation). The fundamental features of the equations of motions are indicated in the formulas for the classical orbital elements

$$
\begin{aligned}
\frac{da}{dt} &= \epsilon f_1 (a, e, i, \omega, \Omega, M) \\
\frac{de}{dt} &= \epsilon f_2 (a, e, i, \omega, \Omega, M) \\
\frac{di}{dt} &= \epsilon f_3 (a, e, i, \omega, \Omega, M) \\
\frac{d\omega}{dt} &= \epsilon f_4 (a, e, i, \omega, \Omega, M) \\
\frac{d\Omega}{dt} &= \epsilon f_5 (a, e, i, \omega, \Omega, M) \\
\frac{dM}{dt} &= n + \epsilon f_6 (a, e, i, \omega, \Omega, M)
\end{aligned}
\qquad (5)
$$

Note that $\epsilon$ is a small parameter related to the magnitude of the perturbing acceleration vector (such as the $J_2$ harmonic coefficient). Therefore, a, e, i, $\omega$, and $\Omega$ are slowly varying elements and M is a fast variable, according to the previous definition.

This formulation is identical to Nayfeh's Generalized Method of Averaging (Reference 7, p. 168) with one exception. In Equation (5), the natural rate of the fast variable is a function of the slow variable a; whereas Nayfeh assumes that the natural rate of the fast variable is a constant.

Following Bogoliubov and Mitropolski,[8] a near identity transformation is assumed:

$$
\begin{aligned}
a &= \bar{a} + \epsilon a_1(\bar{a}, \bar{e}, \bar{i}, \bar{\omega}, \bar{\Omega}, \bar{M}) + \cdots \\
e &= \bar{e} + \epsilon e_1(\bar{a}, \bar{e}, \bar{i}, \bar{\omega}, \bar{\Omega}, \bar{M}) + \cdots \\
i &= \bar{i} + \epsilon i_1(\bar{a}, \bar{e}, \bar{i}, \bar{\omega}, \bar{\Omega}, \bar{M}) + \cdots \\
\omega &= \bar{\omega} + \epsilon \omega_1(\bar{a}, \bar{e}, \bar{i}, \bar{\omega}, \bar{\Omega}, \bar{M}) + \cdots \\
\Omega &= \bar{\Omega} + \epsilon \Omega_1(\bar{a}, \bar{e}, \bar{i}, \bar{\omega}, \bar{\Omega}, \bar{M}) + \cdots \\
M &= \bar{M} + \epsilon M_1(\bar{a}, \bar{e}, \bar{i}, \bar{\omega}, \bar{\Omega}, \bar{M}) + \cdots
\end{aligned}
\qquad (6)
$$

such that the transform of Equation (5) is

$$
\begin{aligned}
\frac{d\bar{a}}{dt} &= \epsilon F_1(\bar{a}, \bar{e}, \bar{i}, \bar{\omega}, \bar{\Omega}) + \cdots \\
\frac{d\bar{e}}{dt} &= \epsilon F_2(\bar{a}, \bar{e}, \bar{i}, \bar{\omega}, \bar{\Omega}) + \cdots \\
\frac{d\bar{i}}{dt} &= \epsilon F_3(\bar{a}, \bar{e}, \bar{i}, \bar{\omega}, \bar{\Omega}) + \cdots \\
\frac{d\bar{\omega}}{dt} &= \epsilon F_4(\bar{a}, \bar{e}, \bar{i}, \bar{\omega}, \bar{\Omega}) + \cdots \\
\frac{d\bar{\Omega}}{dt} &= \epsilon F_5(\bar{a}, \bar{e}, \bar{i}, \bar{\omega}, \bar{\Omega}) + \cdots \\
\frac{d\bar{M}}{dt} &= \bar{n} + \epsilon F_6(\bar{a}, \bar{e}, \bar{i}, \bar{\omega}, \bar{\Omega}) + \cdots
\end{aligned}
\qquad (7)
$$

To determine expressions for the functions $F_1$ through $F_6$ in terms of the known functions $f_1$ through $f_6$, Equations (6) are differentiated with respect to time. Equations (7) are substituted into these expressions and the resulting equations are substituted for the left-hand sides of Equations (5). In addition, Equations (6) are substituted into the right-hand sides of Equations (5). Expanding and equating coefficients of $\epsilon$, equations of the form

$$F_1(\bar{a}, \bar{e}, \bar{i}, \bar{\omega}, \bar{\Omega}) + \bar{n}\frac{\partial}{\partial \bar{M}} a_1(\bar{a}, \cdots, \bar{M}) = f_1(\bar{a}, \cdots, \bar{M}) \qquad (8)$$

are obtained for the slow variables. The quantity $f_1$ is assumed to be the sum of $f_1^s$ (short-period term) and $f_1^\ell$ (long-period term that does not contain the phase angle M). Substitution of the definitions for $f_1^s$ and $f_1^\ell$ into Equation (8) results in

$$F_1 + \bar{n}\frac{\partial}{\partial \bar{M}} a_1 = f_1^s + f_1^\ell \qquad (9)$$

Integration over the period (noting that $a_1$ is periodic in the phase angle) yields the following result:

$$F_1 = \frac{1}{2\pi}\int_0^{2\pi} f_1^\ell \, d\bar{M} \qquad (10)$$

For convenience, $F_1$ can also be written as

$$F_1 = \frac{1}{2\pi}\int_0^{2\pi} f_1 \, d\bar{M} \qquad (11)$$

For the phase angle $\bar{M}$, the following equation is obtained:

$$F_6 + \bar{n} \frac{\partial M_1}{\partial \bar{M}} = f_6 + n_1 \tag{12}$$

where the constraint $n^2 a^3 = \mu$ implies the expansion

$$n = \bar{n} + \epsilon n_1(\bar{a}, \bar{e}, \bar{i}, \bar{\omega}, \bar{\Omega}, \bar{M}) + \cdots \tag{13}$$

After integration over the period of the system, the following equation is obtained:

$$F_6 = \frac{1}{2\pi} \int_0^{2\pi} f_6 \, d\bar{M} \tag{14}$$

Substitution of Equation (11) for $F_1$, the analogous results for the remaining slow variables, and Equation (14) for $F_6$ into Equations (7) give the first-order averaged equations of motion:

$$\begin{aligned}
\frac{d\bar{a}}{dt} &= \frac{1}{2\pi} \int_0^{2\pi} \epsilon f_1(\bar{a}, \bar{e}, \cdots, \bar{M}) \, d\bar{M} \\
\frac{d\bar{e}}{dt} &= \frac{1}{2\pi} \int_0^{2\pi} \epsilon f_2(\bar{a}, \cdots, \bar{M}) \, d\bar{M} \\
\frac{d\bar{i}}{dt} &= \frac{1}{2\pi} \int_0^{2\pi} \epsilon f_3(\bar{a}, \cdots, \bar{M}) \, d\bar{M} \\
\frac{d\bar{\omega}}{dt} &= \frac{1}{2\pi} \int_0^{2\pi} \epsilon f_4(\bar{a}, \cdots, \bar{M}) \, d\bar{M} \\
\frac{d\bar{\Omega}}{dt} &= \frac{1}{2\pi} \int_0^{2\pi} \epsilon f_5(\bar{a}, \cdots, \bar{M}) \, d\bar{M} \\
\frac{d\bar{M}}{dt} &= \bar{n} + \frac{1}{2\pi} \int_0^{2\pi} \epsilon f_6(\bar{a}, \cdots, \bar{M}) \, d\bar{M}
\end{aligned} \tag{15}$$

Equations (15) are the basis of the first-order averaging methods that have been widely applied to orbital prediction problems. This method can be extended to higher order effects. Nayfeh[7] presents an extensive reference list in this area.

Analytical Averaging Methods

For the conservative forces, the perturbed portion of the right-hand sides of Equations (5) can be expressed as a sum of products of the Poisson brackets and the partial derivatives of the perturbing potential (see Appendix A for derivation):

$$\epsilon f_i = -\sum_{j=1}^{6} (a_i, a_j) \frac{\partial R}{\partial a_j} \tag{16}$$

where $a_i$ is now the ith orbital element. Because the Poisson brackets depend only on the slow variables (for the classical orbital elements to be discussed in this section and for the nonsingular variables to be considered in the next section), substitution of Equation (16) into Equations (15) results in

$$\frac{d\bar{a}_i}{dt} = -\sum_{j=1}^{6} (\bar{a}_i, \bar{a}_j) \left[ \frac{1}{2\pi} \int_0^{2\pi} \frac{\partial R}{\partial \bar{a}_j} \, d\bar{M} \right] \tag{17}$$

However, under the assumptions that R and $\partial R/\partial \bar{a}_j$ are continuous, the partial derivative and the integral sign in Equation (17) can be interchanged.[9] The resulting expression is

$$\frac{d\bar{a}_i}{dt} = -\sum_{j=1}^{6} (\bar{a}_i, \bar{a}_j) \frac{\partial}{\partial \bar{a}_j} \left[ \frac{1}{2\pi} \int_0^{2\pi} R \, d\bar{M} \right] \tag{18}$$

Thus, only the perturbing potential must be averaged, not each equation of motion as implied by Equations (15). This simplification explains the connection between conservative perturbations and analytical averaging exhibited in current applications.

An alternative to Equation (16) is the Gaussian form of the VOP equations (see Appendix A for derivation):

$$\epsilon f_i = \frac{\partial a_i}{\partial \dot{\vec{x}}} \cdot \vec{Q} \tag{19}$$

Substitution of Equation (19) into Equations (15) gives

$$\frac{d\bar{a}_i}{dt} = \frac{1}{2\pi} \int_0^{2\pi} \frac{\partial \bar{a}_i}{\partial \dot{\vec{x}}} \cdot \vec{Q} \, d\bar{M} \tag{20}$$

This form for the averaged equations of motion has the advantage of being valid for nonconservative, as well as for conservative, forces.

A first inspection of Equation (20) does not indicate the problems encountered in obtaining closed form expressions for the right-hand sides. Unfortunately, the two-body partial derivatives are functions of the phase angle $\bar{M}$ and must be included in the evaluation of the integral. Also, for some perturbations (such as atmospheric drag), the products $(\partial \bar{a}_i/\partial \dot{\vec{x}}) \cdot \vec{Q}$ are not available as functions of the slowly varying elements.[10] For these perturbations, the perturbing acceleration is a function of the Cartesian coordinates and velocities. Thus, the two-body mechanics are required for the transformation from the slowly varying elements.

Numerical Averaging Methods

Equation (20) is the basis of numerical averaging methods in which the integral in the right-hand side is computed by numerical quadrature methods at each point where the derivative $d\bar{a}_i/dt$ is required. This method has the advantage that the long-term effect of any perturbing acceleration that can be deterministically modeled can be computed.

From the point of view of a system designer who wishes to modify an existing orbit generation program to do averaged orbit generation, application of Equation (20) in a numerical averaging procedure is particularly attractive. It appears that only a quadrature routine is required to interface with usually existing routines for computing $[\partial a_i/\partial \dot{\vec{x}}] \cdot \vec{Q}$. However, for orbits strongly perturbed by atmospheric drag or solar radiation pressure, it is advantageous to consider the near discontinuities in the perturbing acceleration within the context of the quadrature process. (See Optimization of Averaging Methods, below, for more discussion on this point.)

Another circumstance deserves some comment. In Equations (5) the functions $f_i$ were assumed to have no significant dependence on time. This assumption is violated if the longitude-dependent terms in the geopotential are included and the satellite orbital period is of the same magnitude as the central body's rotational period. The assumption is also violated in the case of the third-body perturbation when the disturbing body's period is of the same magnitude as the satellite orbital period. Mathematically, the perturbing acceleration $\vec{Q}$ now depends on two phase angles:

$$\vec{Q} = \vec{Q}(a, e, i, \omega, \Omega, M, M') \tag{21}$$

If M' can be expressed as a function of M, then the previously discussed theory will apply. As a simple example, assume that the two phase angles are governed by the unperturbed solutions

$$M = M_0 + nt \tag{22}$$

$$M' = M'_0 + n't \tag{23}$$

which gives

$$M' = \frac{n'}{n} M + M'_0 - \frac{n'}{n} M_0 \tag{24}$$

Substitution of Equation (24) into Equation (21) converts $\vec{Q}$ into a function of only the slowly varying elements and M. This approach has been taken in the applications with success. Some improvement in the dynamical properties of the averaged equations of motion is noted if the averaging interval corresponds to an integer multiple of the periods associated with both M and M'.

Requirements for Two-Body Results

Consideration of Equations (18) and (20) shows that the following two-body results are required:

1. A transformation from position and velocity to the slowly varying elements and phase angle
2. A transformation from the slowly varying elements and phase angle to position and velocity
3. Poisson brackets for the slowly varying elements and phase angle
4. Partial derivatives of the slowly varying elements and phase angle with respect to velocity

Transformations 1 and 2 are well known for the classical orbital elements. The Poisson brackets for the classical elements are given in References 11 and 12. The partial derivatives of elements with respect to velocity are available in the orbital coordinates, radial coordinates, and tangential coordinates.[12, 13]

Additional two-body results are required for the coefficients of the differential equations that govern the partial derivatives of the mean elements with respect to mean elements at some different epoch.

Application Programs in Classical Elements

Several averaged orbit generation programs based on the classical orbital element formulation have been reported in the literature. Their significant features are described in Table 7. A pattern of treating the zonals and third-body effects via the analytical averaging procedure can be observed. Thus, emphasis is placed on the derivation of the averaged potential. Kaufman's derivation of the third-body potential by use of machine-automated algebra is particularly interesting.[13] Kaufman also tries to take into account the third-body motion during the averaging period via a low-order Taylor series expansion in mean anomaly. The subject of third-body perturbations has also been addressed recently by Kozai[19] and Giacaglia.[20] Certain numerical questions seem to remain open. For example, what is the physical effect of truncating the third-body potential at some low order? What is the effect of the motion of the third body during the averaging interval on the solution?

Cook's paper[15] is interesting because it makes clear the connection between the formulation of the analytically averaged equations of motion and the inclination function, $F_{\ell mp}(i)$ and the Hansen coefficients, which are polynomials in the eccentricity. Later in this paper, when averaging methods expressed in nonsingular variables are considered, it will be reasonable to inquire about the analogous functions in nonsingular variables.

In addition to the work noted above, there have been investigations of long-term orbit prediction problems with resonance conditions that make use of numerical averaging techniques.[21, 22] Finally, several investigators have applied averaged orbit generation processes in differential correction applications.[23-29]

Averaged Orbit Generation in Equinoctial Elements

The variation-of-parameters (unaveraged) equations for the classical orbital elements are singular for small eccentricities and small and near-180-degree inclinations. The practical effect of these singularities is to cause rapid oscillations in some of the orbital elements when the orbit is in a near-singular condition. These oscillations are detrimental both in orbit prediction processes and in statistical orbit determination processes that require orbital predictions. A theoretical basis for the effects of singularities on differential correction processes is developed in Reference 32.

After the equations of motion are averaged, these singularities remain; however, the frequency of the rapid oscillations in the elements depends on the orbit type and the perturbing acceleration model. The degree of difficulty arising from these oscillations also depends on the particular application. For example, with a 24-hour geosynchronous communication satellite, a very rapid motion in the longitude of the ascending node occurs once every 54 years,[33] concurrent with the time of minimum orbital inclination. This motion is significant because the low inclination portion of the long-term history is usually chosen as the active satellite lifetime to take advantage of "passive" stationkeeping properties.

With the Radio Astronomy Explorer-B satellite in a near-circular lunar orbit, many rapid oscillations occur in the argument of perigee over the 1-year lifetime due to the low orbital eccentricity. To predict this orbit with accuracy (using the classical element formulation), a variable-stepsize integration process is required. Alternatively, a fixed-step integration process can be used with a very small stepsize. Both of these procedures are unnecessarily inefficient.

For the determination of mean elements, it might be possible to avoid the rapid oscillations by restricting the observation data span. In this case, the method of averages with classical elements could be used. However, long-term predictions made with the same prediction process using these elements would face the problem described previously. In addition for applications such as gravitational model development,[29] emphasis is on using long arcs of data, and it is not convenient to restrict the data span.

These singularities can be eliminated from the VOP equations by a reasonable transformation to another set of elements. Several possible modifications to the element set are given in Reference 32. In general, each of these modified sets addresses a specific singularity; thus, there is a low eccentricity set, a low inclination set, and a combined low eccentricity/low inclination set. Some of the modified sets cause difficulties with the 90-degree inclination.

The equinoctial elements[34] have the advantage that the partial derivatives of position and velocity with respect to the elements, the Lagrange brackets, the Poisson brackets, and the partial derivatives of the elements with respect to position and velocity are all free from singularities for zero eccentricities and 0- and 90-degree inclinations. Reference 35 introduced the retrograde equinoctial elements, which are free from singularities for zero eccentricities and 90- and 180-degree inclinations. All equations in the direct and retrograde equinoctial elements have the same form except for interchanges of plus and minus signs. This similarity greatly simplifies the development of an averaging method that is applicable to all closed satellite orbits. Finally, Reference 36 provides a brief comparison of equinoctial elements and a low inclination set for differential orbit corrections.

The authors have implemented averaged VOP orbit generation procedures in two programs--the Earth Satellite Mission Analysis Program (ESMAP) and the Goddard Trajectory Determination System (GTDS). ESMAP is an orbit generation program that was built for the mission analysis group at Goddard Space Flight Center (GSFC). In this program, the averaging process is based on the following form of the VOP equations of motion:

$$\frac{da_\alpha}{dt} = -\sum_{\beta=1}^{6} (a_\alpha, a_\beta)\frac{\partial R}{\partial a_\beta} + \frac{\partial a_\alpha}{\partial \dot{\vec{x}}} \cdot \vec{Q} \tag{25}$$

where R = perturbing potential due to the conservative forces

Q = perturbing acceleration for the nonconservative forces

For this application, the perturbing potential R includes the third-body and oblateness effects, and the perturbing acceleration $\vec{Q}$ includes the drag effects and, optionally, the lunar effect. A hybrid averaging procedure has been implemented. The averaged element rates arising from the conservative forces are computed analytically according to Equation (18). The averaged element rates arising from the nonconservative forces are computed numerically according to Equation (20).

GTDS is an operational orbit determination system also supported by GSFC. In this program, a totally numerical averaging procedure is implemented. The averaging equations of motion are in the form given in Equation (20), where all the perturbing forces are included in the evaluation of the perturbing acceleration. Consideration of Equations (18) and (20) shows that the following two-body formulas are required:

1. A transformation from classical elements to equinoctial elements
2. A transformation from position and velocity to equinoctial elements
3. A transformation from the equinoctial elements to position and velocity
4. Poisson brackets for the equinoctial elements
5. Partial derivatives of the equinoctial elements with respect to velocity

These are developed in Appendix B.

In the following paragraphs, the perturbing potentials for third-body effects and oblateness will be developed in equinoctial elements.

## Third-Body Potential†

This paragraph presents the equations for the single-averaged perturbing potential arising from a third body in terms of the equinoctial orbit elements. The partial derivatives of the potential with respect to the equinoctial elements have been generated and the resulting variation-of-parameters (VOP) equations are presented.

The potential employed to model the influence of the Moon and Sun on an Earth satellite is expressed by

$$F^3 = \sum_{n=2}^{\infty} F_n^3 \tag{26}$$

where

$$F_n^3 = \frac{\mu_3}{R_3}\left(\frac{r}{R_3}\right)^n P_n(\cos\psi) \tag{27}$$

In the above expressions

$\mu_3$ = gravitational constant of the third body

$R_3$ = distance from the central body to the third body

$r$ = distance from the central body to the satellite

$P_n$ = Legendre polynomial of nth order

$\psi$ = angle between the vectors $\vec{r}$ and $\vec{R}_3$

If the final equations are to be accurate to the sixth order in the ratio of the satellite distance to the third-body distance, the $P_n(\cos\psi)$ for n = 2, 3, 4, 5, and 6 are required.

In the present development, the argument $\cos\psi$ can be expressed as

$$\cos\psi = \alpha_1 \cos L + \beta_1 \sin L \tag{28}$$

where L is the true longitude defined in Equation (B-21) and

$$\begin{aligned} \alpha_1 &= \hat{f} \cdot \hat{R}_3 \\ \beta_1 &= \hat{g} \cdot \hat{R}_3 \\ \gamma_1 &= \hat{w} \cdot \hat{R}_3 \end{aligned} \tag{29}$$

are the direction cosines of the third body relative to the equinoctial frame (Figure 4). The quantity $\hat{R}_3$ is a unit vector from the central body to the third body. Equations (28) and (29) are valid only for the direct equinoctial orbit elements. For the retrograde case, the argument $\cos\psi$ has the form

$$\cos\psi = \alpha_r \cos L^* + \beta_r \sin L^* \tag{30}$$

where L* is the retrograde true longitude defined in Equation (B-35) and

$$\begin{aligned} \alpha_r &= \hat{f}^* \cdot \hat{R}_3 \\ \beta_r &= \hat{g}^* \cdot \hat{R}_3 \\ \gamma_r &= \hat{w}^* \cdot \hat{R}_3 \end{aligned} \tag{31}$$

are the direction cosines relative to the retrograde coordinate frame ( f*, g*, w*) (Figure 5). The resulting expressions for the $P_n(\cos\psi)$ are

$$\begin{aligned} P_2(\cos\psi) &= \frac{1}{2}\left[\frac{3}{2}S_2 + \frac{3}{2}S_3 \cos 2L + 3S_1 \sin 2L - 1\right] \\ P_3(\cos\psi) &= \frac{1}{2}\left[\frac{5}{4}\alpha_1 S_4 \cos 3L - \frac{5}{4}\beta_1 S_5 \sin 3L \right. \\ &\quad \left. + 3\alpha_1\left(\frac{5}{4}S_2 - 1\right)\cos L + 3\beta_1\left(\frac{5}{4}S_2 - 1\right)\sin L\right] \\ P_4(\cos\psi) &= \frac{1}{64}\left[105S_2^2 - 120S_2 + 24 \right. \\ &\quad + 35\left(S_3^2 - 4S_1^2\right)\cos 4L + 140S_1S_3 \sin 4L \\ &\quad \left. + 20S_3(7S_2 - 6)\cos 2L + 40S_1(7S_2 - 6)\sin 2L\right] \end{aligned} \tag{32}$$

† See Reference 37 for a more complete description of this work.

$$
\begin{aligned}
P_5(\cos\psi) = \frac{63}{128}\Big[&\alpha_1\left(S_8^2 - 20\beta_1^4\right)\cos 5L \\
&+ \beta_1\left(S_9^2 - 20\alpha_1^4\right)\sin 5L \\
&+ 5\alpha_1\left(S_3^2 - 4\beta_1^4 - \frac{8}{9}S_4\right)\cos 3L \\
&- 5\beta_1\left(S_3^2 - 4\alpha_1^4 - \frac{8}{9}S_5\right)\sin 3L \\
&+ 10\alpha_1\left(S_2^2 - \frac{4}{3}S_2 + \frac{8}{21}\right)\cos L \\
&+ 10\beta_1\left(S_2^2 - \frac{4}{3}S_2 + \frac{8}{21}\right)\sin L\Big]
\end{aligned}
\qquad \begin{matrix}(32)\\ \text{(Cont'd)}\end{matrix}
$$

$$
\begin{aligned}
P_6(\cos\psi) = \frac{231}{256}\Big[&5\left(S_2^3 - \frac{18}{11}S_2^2 + \frac{8}{11}S_2 - \frac{16}{231}\right) \\
&+ \frac{1}{2}S_3\left(S_{10}^2 - 48\beta_1^4\right)\cos 6L \\
&+ 3S_1\left(S_3^2 - \frac{4}{3}S_1^2\right)\sin 6L \\
&+ 3\left(S_4^2 - 8\beta_1^4\right)\left(S_2 - \frac{10}{11}\right)\cos 4L \\
&+ 12S_1S_3\left(S_2 - \frac{10}{11}\right)\sin 4L \\
&+ 5S_3\left(\frac{3}{2}S_2^2 - \frac{24}{11}S_2 + \frac{8}{11}\right)\cos 2L \\
&+ 5S_1\left(3S_2^2 - \frac{48}{11}S_2 + \frac{16}{11}\right)\sin 2L\Big]
\end{aligned}
$$

where the auxiliary variables $S_1, \cdots, S_{10}$ are given by

$$
\begin{aligned}
S_1 &= \alpha_1\beta_1 \\
S_2 &= \alpha_1^2 + \beta_1^2 \\
S_3 &= \alpha_1^2 - \beta_1^2 \\
S_4 &= \alpha_1^2 - 3\beta_1^2 \\
S_5 &= \beta_1^2 - 3\alpha_1^2 \\
S_6 &= 4\beta_1^2(2\alpha_1^2 - \beta_1^2) \\
S_7 &= 4\alpha_1^2(2\beta_1^2 - \alpha_1^2) \\
S_8 &= \alpha_1^2 - 5\beta_1^2 \\
S_9 &= \beta_1^2 - 5\alpha_1^2
\end{aligned}
\qquad (33)
$$

$$
S_{10} = \alpha_1^2 - 7\beta_1^2 \qquad \begin{matrix}(33)\\ \text{(Cont'd)}\end{matrix}
$$

These expressions are for the direct equinoctial orbit elements. Because Equation (30) for the retrograde case has the same form as Equation (28) for the direct elements, it follows that all generated results can be applied directly, provided one makes the transformation

$$
\begin{aligned}
L &\rightarrow L^* \\
\alpha_1 &\rightarrow \alpha_r \\
\beta_1 &\rightarrow \beta_r
\end{aligned}
\qquad (34)
$$

The potential is averaged over the period of the orbit according to

$$
\bar{F}^3 = \frac{1}{2\pi}\int_0^{2\pi} F^3\, d\lambda \qquad (35)
$$

Inserting Equations (26) and (27) into the above gives

$$
F^3 = \frac{1}{2\pi}\frac{\mu_3}{R_3}\sum_{n=2}^{6}\left(\frac{a}{R_3}\right)^n \int_0^{2\pi}\left(\frac{r}{a}\right)^n P_n(\cos\psi)\, dM \qquad (36)
$$

The integrals in Equation (36) are evaluated via use of Hansen's coefficients.[38] An extensive table of the Hansen coefficients expressed in terms of the equinoctial variables is given in Reference 37. The resulting averaged potentials are:

$$
\bar{F}_2^3 = \frac{\mu_3}{2R_3}\left(\frac{a}{R_3}\right)^2\left[A_1B_1 + 15\left(S_1V_1 + \frac{1}{4}S_3V_3\right)\right] \qquad (37)
$$

$$
\begin{aligned}
\bar{F}_3^3 = \frac{25\mu_3}{8R_3}\left(\frac{a}{R_3}\right)^3\Big[&\frac{7}{8}A_2B_2 + \frac{7}{8}A_3B_3 \\
&+ \frac{6}{5}A_4B_4(\alpha_1 k + \beta_1 h)\Big]
\end{aligned}
\qquad (38)
$$

$$
\begin{aligned}
\bar{F}_4^3 = \frac{\mu_3}{64R_3}\left(\frac{a}{R_3}\right)^4\Big[&A_5B_5 - \frac{2205}{8}A_6B_6 + 4410A_7B_7 \\
&+ \frac{105}{2}A_8B_8(S_3V_3 + 4S_1V_1)\Big]
\end{aligned}
\qquad (39)
$$

$$
\begin{aligned}
\bar{F}_5^3 = \frac{63\mu_3}{128R_3}\left(\frac{a}{R_3}\right)^5\Big[&-\frac{231}{16}A_9B_9 - \frac{231}{16}A_{10}B_{10} \\
&- \frac{105}{16}A_{11}B_{11} + \frac{105}{16}A_{12}B_{12} \\
&- 35A_{13}B_{13}(\alpha_1 k + \beta_1 h)\Big]
\end{aligned}
\qquad (40)
$$

$$\overline{F}_6^3 = \frac{231\mu_3}{256R_3}\left(\frac{a}{R_3}\right)^6 \left[\frac{5}{3696} A_{14}B_{14} + \frac{429}{32} A_{15}B_{15} + \frac{429}{8} A_{16}B_{16} + \frac{297}{16} A_{17}B_{17} + 297 A_{18}B_{18} + \frac{135}{2} A_{19}B_{19} + 270 A_{20}B_{20}\right] \tag{41}$$

*where the auxiliary Vs are*

$$\begin{aligned} V_1 &= hk \\ V_2 &= h^2 + k^2 \\ V_3 &= k^2 - h^2 \\ V_4 &= k^2 - 3h^2 \\ V_5 &= 3k^2 - h^2 \\ V_6 &= 4h^2\ (2k^2 - h^2) \\ V_7 &= 4k^2\ (2h^2 - k^2) \end{aligned} \tag{42}$$

and the As and Bs are given in Table 8.

Considering the disturbing functions given in Equations (37) through (41) as well as the auxiliary quantities given in Equation (33), Equation (42), and Table 8, it is clear that

$$\overline{F}_i^3 = R\,(a,\ \alpha_1,\ \beta_1,\ h,\ k) \tag{43}$$

The partial derivatives with respect to h and k can be taken in a straightforward manner. For the variations with respect to p and q, further analysis is required. In particular

$$\frac{\partial R}{\partial p} = \frac{\partial R}{\partial \alpha_1}\frac{\partial \alpha_1}{\partial p} + \frac{\partial R}{\partial \beta_1}\frac{\partial \beta_1}{\partial p} \tag{44}$$

and

$$\frac{\partial R}{\partial q} = \frac{\partial R}{\partial \alpha_1}\frac{\partial \alpha_1}{\partial q} + \frac{\partial R}{\partial \beta_1}\frac{\partial \beta_1}{\partial q} \tag{45}$$

Going back to Equation (29), it follows that

$$\begin{aligned} \frac{\partial \alpha_1}{\partial p} &= \frac{\partial \hat{f}}{\partial p}\cdot \hat{R}_3 \\ \frac{\partial \alpha_1}{\partial q} &= \frac{\partial \hat{f}}{\partial q}\cdot \hat{R}_3 \end{aligned} \tag{46}$$

$$\begin{aligned} \frac{\partial \beta_1}{\partial p} &= \frac{\partial \hat{g}}{\partial p}\cdot \hat{R}_3 \\ \frac{\partial \beta_1}{\partial q} &= \frac{\partial \hat{g}}{\partial q}\cdot \hat{R}_3 \end{aligned}$$

so that

$$\begin{aligned} \frac{\partial \alpha_1}{\partial p} &= \frac{-2}{(1+p^2+q^2)}\left[q\beta_1 I + \gamma_1\right] \\ \frac{\partial \alpha_1}{\partial q} &= \frac{2I}{(1+p^2+q^2)}\,p\beta_1 \\ \frac{\partial \beta_1}{\partial p} &= \frac{2I}{(1+p^2+q^2)}\,q\alpha_1 \\ \frac{\partial \beta_1}{\partial q} &= \frac{-2I}{(1+p^2+q^2)}\left[p\alpha_1 - \gamma_1\right] \end{aligned} \tag{47}$$

Returning to the VOP equations, it is seen that these equations contain the term

$$p\frac{\partial R}{\partial p} + q\frac{\partial R}{\partial q} \tag{48}$$

Employing Equations (44) and (45) for $\partial R/\partial p$ and $\partial R/\partial q$ with Equations (47) allows one to write

$$p\frac{\partial R}{\partial p} + q\frac{\partial R}{\partial q} = \frac{-2\gamma_1}{(1+p^2+q^2)}\left(p\frac{\partial R}{\partial \alpha_1} - q\frac{\partial R}{\partial \beta_1} I\right) \tag{49}$$

Employing the identity

$$k\frac{\partial R}{\partial h} - h\frac{\partial R}{\partial k} - \beta_1\frac{\partial R}{\partial \alpha_1} + \alpha_1\frac{\partial R}{\partial \beta_1} = 0 \tag{50}$$

the VOP equations adopt the form

$$\frac{da}{dt} = 0 \tag{51}$$

$$\frac{dh}{dt} = \frac{1}{na^2\sqrt{1-h^2-k^2}}\left[(1-h^2-k^2)\frac{\partial R}{\partial k} - k\gamma_1\left(p\frac{\partial R}{\partial \alpha_1} - q\frac{\partial R}{\partial \beta_1} I\right)\right] \tag{52}$$

$$\frac{dk}{dt} = \frac{-1}{na^2\sqrt{1-h^2-k^2}}\left[(1-h^2-k^2)\frac{\partial R}{\partial h} - h\gamma_1\left(p\frac{\partial R}{\partial \alpha_1} - q\frac{\partial R}{\partial \beta_1} I\right)\right] \tag{53}$$

$$\frac{dp}{dt} = \frac{(1+p^2+q^2)}{2na^2\sqrt{1-h^2-k^2}}\,\gamma_1\frac{\partial R}{\partial \beta_1} \tag{54}$$

$$\frac{dq}{dt} = \frac{(1+p^2+q^2)I}{2na^2\sqrt{1-h^2-k^2}}\gamma_1\frac{\partial R}{\partial \alpha_1} \tag{55}$$

Adopting the convention

$$R \rightarrow \bar{F}_i^3$$

to obtain the final form for the VOP equations, the partial *derivatives*

$$\frac{\partial \bar{F}_i^3}{\partial h},\ \frac{\partial \bar{F}_i^3}{\partial k},\ \frac{\partial \bar{F}_i^3}{\partial \alpha_1},\ \frac{\partial \bar{F}_i^3}{\partial \beta_1} \tag{56}$$

must be generated.

Inspection of Equation (33), the $S_i$s, Equation (42), the $V_i$s, and Table 8, the $A_i$s and $B_i$s, yields directly that

$$\begin{aligned}
&\frac{\partial A_i}{\partial h} = \frac{\partial A_i}{\partial k} = \frac{\partial S_i}{\partial h} = \frac{\partial S_i}{\partial k} \equiv 0 \\
&\frac{\partial B_i}{\partial \alpha_1} = \frac{\partial B_i}{\partial \beta_1} = \frac{\partial V_i}{\partial \alpha_1} = \frac{\partial V_i}{\partial \beta_1} \equiv 0
\end{aligned} \tag{57}$$

and the relevant equations are:

$\bar{F}_2^3$ Derivatives

$$\begin{aligned}
\frac{\partial \bar{F}_2^3}{\partial k} &= \frac{\mu_3}{2R_3}\left(\frac{a}{R_3}\right)^2\left[A_1\frac{\partial B_1}{\partial k} + 15\left(hS_1 + \frac{1}{2}kS_3\right)\right] \\
\frac{\partial \bar{F}_2^3}{\partial h} &= \frac{\mu_3}{2R_3}\left(\frac{a}{R_3}\right)^2\left[A_1\frac{\partial B_1}{\partial h} + 15\left(kS_1 - \frac{1}{2}hS_3\right)\right] \\
\frac{\partial \bar{F}_2^3}{\partial \alpha_1} &= \frac{\mu_3}{2R_3}\left(\frac{a}{R_3}\right)^2\left[\frac{\partial A_1}{\partial \alpha_1}B_1 + 15\left(\beta_1 V_1 + \frac{1}{2}\alpha_1 V_3\right)\right] \\
\frac{\partial \bar{F}_2^3}{\partial \beta_1} &= \frac{\mu_3}{2R_3}\left(\frac{a}{R_3}\right)^2\left[\frac{\partial A_1}{\partial \beta_1}B_1 + 15\left(\alpha_1 V_1 - \frac{1}{2}\beta_1 V_3\right)\right]
\end{aligned} \tag{58}$$

$\bar{F}_3^3$ Derivatives

$$\begin{aligned}
\frac{\partial \bar{F}_3^3}{\partial k} = \frac{25\mu_3}{8R_3}\left(\frac{a}{R_3}\right)^3\Bigg[&\frac{7}{8}A_2\frac{\partial B_2}{\partial k} + \frac{7}{8}A_3\frac{\partial B_3}{\partial k} \\
&+ \frac{6}{5}\alpha_1 A_4 B_4 + \frac{6}{5}A_4(\alpha_1 k + \beta_1 h)\frac{\partial B_4}{\partial k}\Bigg]
\end{aligned} \tag{59}$$

$$\begin{aligned}
\frac{\partial \bar{F}_3^3}{\partial h} = \frac{25\mu_3}{8R_3}\left(\frac{a}{R_3}\right)^3\Bigg[&\frac{7}{8}A_2\frac{\partial B_2}{\partial h} + \frac{7}{8}A_3\frac{\partial B_3}{\partial h} \\
&+ \frac{6}{5}\beta_1 A_4 B_4 + \frac{6}{5}A_4(\alpha_1 k + \beta_1 h)\frac{\partial B_4}{\partial h}\Bigg] \\
\frac{\partial \bar{F}_3^3}{\partial \alpha_1} = \frac{25\mu_3}{8R_3}\left(\frac{a}{R_3}\right)\Bigg[&\frac{7}{8}\frac{\partial A_2}{\partial \alpha_1}B_2 + \frac{7}{8}\frac{\partial A_3}{\partial \alpha_1}B_3 \\
&+ \frac{6}{5}kA_4B_4 + \frac{6}{5}B_4(\alpha_1 k + \beta_1 h)\frac{\partial A_4}{\partial \alpha_1}\Bigg] \\
\frac{\partial \bar{F}_3^3}{\partial \beta_1} = \frac{25\mu_3}{8R_3}\left(\frac{a}{R_3}\right)^3\Bigg[&\frac{7}{8}\frac{\partial A_2}{\partial \beta_1}B_2 + \frac{7}{8}\frac{\partial A_3}{\partial \beta_1}B_3 \\
&+ \frac{6}{5}hA_4B_4 + \frac{6}{5}B_4(\alpha_1 k + \beta_1 h)\frac{\partial A_4}{\partial \beta_1}\Bigg]
\end{aligned} \tag{59 (Cont'd)}$$

$\bar{F}_4^3$ Derivatives

$$\begin{aligned}
\frac{\partial \bar{F}_4^3}{\partial k} = \frac{\mu_3}{64R_3}\left(\frac{a}{R_3}\right)^4\Bigg[&A_5\frac{\partial B_5}{\partial k} + \frac{2205}{8}A_6\frac{\partial B_6}{\partial k} \\
&+ 4410\,A_7\frac{\partial B_7}{\partial k} + \frac{105}{2}A_8(4S_1V_1 \\
&+ S_3V_3)\frac{\partial B_8}{\partial k} + 105\,A_8B_8(2hS_1 + kS_3)\Bigg] \\
\frac{\partial \bar{F}_4^3}{\partial h} = \frac{\mu_3}{64R_3}\left(\frac{a}{R_3}\right)^4\Bigg[&A_5\frac{\partial B_5}{\partial h} + \frac{2205}{8}A_6\frac{\partial B_6}{\partial h} \\
&+ 4410\,A_7\frac{\partial B_7}{\partial h} + \frac{105}{2}A_8(4S_1V_1 \\
&+ S_3V_3)\frac{\partial B_8}{\partial h} + 105\,A_8B_8(2kS_1 - hS_3)\Bigg] \\
\frac{\partial \bar{F}_4^3}{\partial \alpha_1} = \frac{\mu_3}{64R_3}\left(\frac{a}{R_3}\right)^4\Bigg[&\frac{\partial A_5}{\partial \alpha_1}B_5 + \frac{2205}{8}\frac{\partial A_6}{\partial \alpha_1}B_6 \\
&+ 4410\frac{\partial A_7}{\partial \alpha_1}B_7 + \frac{105}{2}B_8(4S_1V_1 \\
&+ S_3V_3)\frac{\partial A_8}{\partial \alpha_1} + 105\,A_8B_8\,(2\beta_1V_1 + \alpha_1V_3)\Bigg]
\end{aligned} \tag{60}$$

$$\frac{\partial \bar{F}_4^3}{\partial \beta_1} = \frac{\mu_3}{64R_3}\left(\frac{a}{R_3}\right)^4 \left[\frac{\partial A_5}{\partial \beta_1} B_5 + \frac{2205}{8}\frac{\partial A_6}{\partial \beta_1} B_6 + 4410 \frac{\partial A_7}{\partial \beta_1} B_7 + \frac{105}{2} B_8 (4S_1V_1 + S_3V_3)\frac{\partial A_8}{\partial \beta_1} + 105 A_8 B_8 (2\alpha_1 V_1 - \beta_1 V_3)\right] \tag{60 (Cont'd)}$$

$\bar{F}_5^3$ Derivatives

$$\frac{\partial \bar{F}_5^3}{\partial k} = -\frac{63\mu_3}{128R_3}\left(\frac{a}{R_3}\right)^5 \left[\frac{231}{16} A_9 \frac{\partial B_9}{\partial k} + \frac{231}{16} A_{10}\frac{\partial B_{10}}{\partial k} + \frac{105}{16} A_{11}\frac{\partial B_{11}}{\partial k} - \frac{105}{8} A_{12}\frac{\partial B_{12}}{\partial k} + 35\alpha_1 A_{13} B_{13} + 35 A_{13}(\alpha_1 k + \beta_1 h)\frac{\partial B_{13}}{\partial k}\right]$$

$$\frac{\partial \bar{F}_5^3}{\partial h} = -\frac{63\mu_3}{128R_3}\left(\frac{a}{R_3}\right)^5 \left[\frac{231}{16} A_9 \frac{\partial B_9}{\partial h} + \frac{231}{16} A_{10}\frac{\partial B_{10}}{\partial h} + \frac{105}{16} A_{11}\frac{\partial B_{11}}{\partial h} - \frac{105}{8} A_{12}\frac{\partial B_{12}}{\partial h} + 35\beta_1 A_{13} B_{13} + 35 A_{13}(\alpha_1 k + \beta_1 h)\frac{\partial B_{13}}{\partial h}\right] \tag{61}$$

$$\frac{\partial \bar{F}_5^3}{\partial \alpha_1} = -\frac{63\mu_3}{128R_3}\left(\frac{a}{R_3}\right)^5 \left[\frac{231}{16}\frac{\partial A_9}{\partial \alpha_1} B_9 + \frac{231}{16}\frac{\partial A_{10}}{\partial \alpha_1} B_{10} + \frac{105}{16}\frac{\partial A_{11}}{\partial \alpha_1} B_{11} - \frac{105}{8}\frac{\partial A_{12}}{\partial \alpha_1} B_{12} + 35 k A_{13} B_{13} + 35 B_{13}(\alpha_1 k + \beta_1 h)\frac{\partial A_{13}}{\partial \alpha_1}\right]$$

$$\frac{\partial \bar{F}_5^3}{\partial \beta_1} = -\frac{63\mu_3}{128R_3}\left(\frac{a}{R_3}\right)^5 \left[\frac{231}{16}\frac{\partial A_9}{\partial \beta_1} B_9 + \frac{231}{16}\frac{\partial A_{10}}{\partial \beta_1} B_{10} + \frac{105}{16}\frac{\partial A_{11}}{\partial \beta_1} B_{11} - \frac{105}{8}\frac{\partial A_{12}}{\partial \beta_1} B_{12} + 35 h A_{13} B_{13} + 35 B_{13}(\alpha_1 k + \beta_1 h)\frac{\partial A_{13}}{\partial \beta_1}\right]$$

$\bar{F}_6^3$ Derivatives

$$\frac{\partial \bar{F}_6^3}{\partial k} = \frac{231\mu_3}{256R_3}\left(\frac{a}{R_3}\right)^6 \left[\frac{5}{3696} A_{14}\frac{\partial B_{14}}{\partial k} + \frac{429}{32} A_{15}\frac{\partial B_{15}}{\partial k} + \frac{429}{8} A_{16}\frac{\partial B_{16}}{\partial k} + \frac{297}{16} A_{17}\frac{\partial B_{17}}{\partial k} + 297 A_{18}\frac{\partial B_{18}}{\partial k} + \frac{135}{2} A_{19}\frac{\partial B_{19}}{\partial k} + 270 A_{20}\frac{\partial B_{20}}{\partial k}\right]$$

$$\frac{\partial \bar{F}_6^3}{\partial h} = \frac{231\mu_3}{256R_3}\left(\frac{a}{R_3}\right)^6 \left[\frac{5}{3696} A_{14}\frac{\partial B_{14}}{\partial h} + \frac{429}{32} A_{15}\frac{\partial B_{15}}{\partial h} + \frac{429}{8} A_{16}\frac{\partial B_{16}}{\partial h} + \frac{297}{16} A_{17}\frac{\partial B_{17}}{\partial h} + 297 A_{18}\frac{\partial B_{18}}{\partial h} + \frac{135}{2} A_{19}\frac{\partial B_{19}}{\partial h} + 270 A_{20}\frac{\partial B_{20}}{\partial h}\right] \tag{62}$$

$$\frac{\partial \bar{F}_6^3}{\partial \alpha_1} = \frac{231\mu_3}{256R_3}\left(\frac{a}{R_3}\right)^6 \left[\frac{5}{3696}\frac{\partial A_{14}}{\partial \alpha_1} B_{14} + \frac{429}{32}\frac{\partial A_{15}}{\partial \alpha_1} B_{15} + \frac{429}{8}\frac{\partial A_{16}}{\partial \alpha_1} B_{16} + \frac{297}{16}\frac{\partial A_{17}}{\partial \alpha_1} B_{17} + 297\frac{\partial A_{18}}{\partial \alpha_1} B_{18} + \frac{135}{2}\frac{\partial A_{19}}{\partial \alpha_1} B_{19} + 270\frac{\partial A_{20}}{\partial \alpha_1} B_{20}\right]$$

$$\frac{\partial \bar{F}_6^3}{\partial \beta_1} = \frac{231\mu_3}{256R_3}\left(\frac{a}{R_3}\right)^6 \left[\frac{5}{3696}\frac{\partial A_{14}}{\partial \beta_1} B_{14} + \frac{429}{32}\frac{\partial A_{15}}{\partial \beta_1} B_{15} + \frac{429}{8}\frac{\partial A_{16}}{\partial B_1} B_{16} + \frac{297}{16}\frac{\partial A_{17}}{\partial \beta_1} B_{17} + 297\frac{\partial A_{18}}{\partial \beta_1} B_{18} + \frac{135}{2}\frac{\partial A_{19}}{\partial \beta_1} B_{19} + 270\frac{\partial A_{20}}{\partial \beta_1} B_{20}\right]$$

The derivatives of $A_i$ and $B_i$ with respect to the relevant variables are obtained from the definitions given in Table 8. These derivatives are also listed in Reference 37.

Oblateness Potential

This paragraph gives the equinoctial variation-of-parameters (VOP) equations for the oblateness potential. The model employed in this analysis consists of the oblateness potential arising from the contributions of the $J_2$, $J_3$, and $J_4$ harmonic coefficient terms. The ensuing contributions to the total VOP equations are given in terms of the nonsingular equinoctial orbit elements, both for direct and retrograde orbits.

The individual contributions to the oblateness potential[39, 40] for the $J_2$, $J_3$, and $J_4$ harmonic coefficient terms, respectively, are

$$\bar{\bar{F}}_{20} = \frac{(1 - e^2)^{3/2}}{4P^3} \left(1 - 3 \cos^2 i\right) \tag{63}$$

$$\bar{\bar{F}}_{30} = \frac{3e\,(1 - e^2)^{3/2}}{2P^4} \sin \omega \sin i \left[\frac{5}{4} \sin^2 i - 1\right] \tag{64}$$

$$\bar{\bar{F}}_{40} = \frac{3(1 - e^2)^{3/2}}{8P^5} \left\{\left(1 + \frac{3}{2} e^2\right) \left(1 - 5 \sin^2 i + \frac{35}{8} \sin^4 i\right) + \frac{5 e^2}{8} \left(6 - 7 \sin^2 i\right) \sin^2 i \cos 2\omega \right\} \tag{65}$$

The quantity P appearing in the above expressions is the *semilatus rectum. These expressions can be trans*formed into corresponding forms in terms of the equinoctial orbit elements by employing the definitions given in Equation (B-1) together with the auxiliary variables

$$\begin{aligned}
b &= 1 - h^2 - k^2 \\
c &= p^2 + q^2 \\
d &= 1 + c \\
\eta_1 &= kp - hqI \\
\eta_2 &= hq - kpI = -\eta_1 I \\
\eta_3 &= hp + kqI
\end{aligned} \tag{66}$$

The symbol I has the meaning given in Appendix B.

Defining the sums

$$\begin{aligned}
S_1 &= 1 - 4c + c^2 \\
S_2 &= 1 - 3c + c^2 \\
S_3 &= 3 - 8c + 3c^2 \\
S_4 &= 7 + 40c + 7c^2 \\
S_5 &= 1 - 16c + 36c^2 - 16c^3 + c^4 \\
S_6 &= 1 + 2c - 3c^2 + 2c^3 + c^4 \\
S_7 &= 1 - 8c + 18c^2 - 8c^3 + c^4
\end{aligned} \tag{67}$$

$$S_8 = 1 - 40c + 40c^2 - 40c^3 + c^4 \tag{67 (Cont'd)}$$

gives rise to the expressions,

for the $J_2$ contribution:

$$\bar{\bar{F}}_{20} = -\frac{S_1}{2a^3 b^{3/2} d^2} \tag{68}$$

for the $J_3$ contribution:

$$\bar{\bar{F}}_{30} = \frac{3\eta_1 S_2}{a^4 b^{5/2} d^3} I \tag{69}$$

for the $J_4$ contribution:

$$\bar{\bar{F}}_{40} = \frac{3}{8a^5 b^{7/2} d^4} \left\{\left(1 + \frac{3}{2} (h^2 + k^2)\right) S_5 + 5\left(\eta_3^2 - \eta_2^2\right) S_3 \right\} \tag{70}$$

The VOP equations for the oblateness potential associated with the $J_2$ harmonic coefficient are

$$\begin{aligned}
\frac{dh}{dt} &= \frac{3\mu R_e^2 J_2\, k\, S_9}{2na^5 b^2 d^2} \\
\frac{dk}{dt} &= -\frac{3\mu R_e^2 J_2\, h\, S_9}{2na^5 b^2 d^2} \\
\frac{dp}{dt} &= -\frac{3\mu R_e^2 J_2\, q\, \bar{d}}{2na^5 b^2 d} I \\
\frac{dq}{dt} &= \frac{3\mu R_e^2 J_2\, p\, \bar{d}}{2na^5 b^2 d} I
\end{aligned} \tag{71}$$

where

$$\begin{aligned}
\bar{d} &= 1 - c \\
S_9 &= 1 - 6c + 3c^2
\end{aligned} \tag{72}$$

These expressions are valid for both the direct and retrograde orbits. For the retrograde case, $I = -1$ must be employed.

The VOP equations for the oblateness potential associated with the $J_3$ harmonic coefficient are

$$\frac{dh}{dt} = -\frac{3\mu R_e^3 J_3}{2na^6 b^3 d^3} I \left\{ 2S_2 (p - h\eta_3 - 4k\eta_2 I) - k\eta_2 \bar{d} S_{10} I \right\}$$

$$\frac{dk}{dt} = -\frac{3\mu R_e^3 J_3}{2na^6 b^3 d^3} \left\{ 2S_2 (q - k\eta_3 + 4h\eta_2) + h\eta_2 \bar{d} S_{10} I \right\}$$

$$\frac{dp}{dt} = \frac{3\mu R_e^3 J_3 \bar{d}}{4na^6 b^3} I \left\{ h - 5 \frac{(p\eta_3 I + 3q\eta_2)}{d^2} \right\}$$

$$\frac{dq}{dt} = \frac{3\mu R_e^3 J_3 \bar{d}}{4na^6 b^3} \left\{ k - 5 \frac{(q\eta_3 I - 3p\eta_2 I)}{d^2} \right\} \tag{73}$$

where

$$S_{10} = 1 - 13c + c^2 \tag{74}$$

The VOP equations for the oblateness potential associated with the $J_4$ harmonic coefficient term are

$$\frac{dh}{dt} = -\frac{15\mu R_e^4 J_4}{16na^7 b^4 d^4} I \left\{ 8\eta_2 (p - h\eta_3) S_3 + k \left[ 4S_{12} + (h^2 + k^2) S_{13} - 4\eta_2^2 S_{14} \right] I \right\}$$

$$\frac{dk}{dt} = -\frac{15\mu R_e^4 J_4}{16na^7 b^4 d^4} \left\{ 8\eta_2 (q - k\eta_3 I) S_3 - h \left[ 4S_{12} + (h^2 + k^2) S_{13} - 4\eta_2^2 S_{14} \right] \right\}$$

$$\frac{dp}{dt} = \frac{15\mu R_e^4 J_4 \bar{d}}{8na^7 b^4 d^3} I \left\{ h\eta_2 S_3 - q \left[ 14\eta_2^2 - \frac{1}{2} (h^2 + k^2) S_3 - S_{15} \right] \right\} \tag{75}$$

$$\frac{dq}{dt} = \frac{15\mu R_e^4 J_4 \bar{d}}{8na^7 b^4 d^3} I \left\{ k\eta_2 S_3 + p \left[ 14\eta_2^2 - \frac{1}{2} (h^2 + k^2) S_3 - S_{15} \right] \right\}$$

where

$$S_{12} = 1 - 15c + 40c^2 - 25c^3 + 3c^4$$

$$S_{13} = 3 - 24c + 50c^2 - 40c^3 + 9c^4$$

$$S_{14} = 18 - 65c + 40c^2 + 3c^3 \tag{76}$$

$$S_{15} = 2(1 - 5c + c^2)$$

Numerical Results

As indicated previously, the accuracy of analytical averaging for third-body perturbations on long-period orbits is unresolved. The remaining questions include:

1. What is the effect of holding the lunar position fixed during the process of averaging the disturbing potential?

2. Do higher order terms in the Legendre expansion improve the results?

To provide some physical insight in these areas, the analytical theories derived in the previous paragraphs have been tested on the NEMD orbit (see Table 1 for initial conditions). The results of this effort are given in Tables 9 and 10. In each case, the heading at the top of the table indicates the smallest term included in the particular simulation. The results of a numerically averaged orbit prediction run were used as a reference.* In all cases the deviations decrease as higher order terms are added. However, the decrease in the error is not a smooth function of the highest order term included. Specifically, the improvement arising from the $(a/R_3)^4$ term is much larger than that from the $(a/R_3)^3$ term. Numerical results for the $(a/R_3)^6$ term are not complete at this time. It seems clear that the higher order terms in the Legendre expansion for the third-body disturbing potential definitely reduce the errors in the analytical averaging process.

Additional results relating to the accuracy of averaging processes are contained in References 37, 41, and 42.

Numerical Integration Procedure

Considerable research has been performed on the problem of determining the most efficient numerical integration procedure for solution of the orbit problem. Multistep predictor-corrector procedures have been shown to be significantly more efficient for this application than single-step methods (Reference 43). In particular, an evaluation of various multistep numerical

* Only the lunar perturbation was numerically averaged. Oblateness and solar perturbations were treated with analytical averaging.

integration formulas (Reference 44) has shown that the Adams-Bashforth predictor and Adams-Moulton corrector formulas are, in general, most efficient for integration of the Class I orbital equations of motion.† For these reasons, multistep Adams integration procedures have been used in our orbit generation subprograms.

To achieve the maximum possible efficiency from an averaged prediction method, care must be taken that the integration stepsize is limited as much as possible by accuracy rather than numerical stability considerations. In maximizing the numerical stability characteristics of an orbit generator, both the numerical integration process and the equations of motion must be considered. The following factors are important in this regard.

1. The integration algorithm
2. The order of the integration formulas
3. Special treatment of discontinuous perturbations

The authors (Reference 41) have evaluated various predictor-corrector algorithms using integration orders ranging from 4th to 11th for integration of the VOP equations of motion, both precision and averaged. For integration of the precision equations of motion, 11th-order integration formulas used in a Predict, Evaluate, Correct, Partial-Evaluate (PECE*) algorithm were found to be most efficient for most applications. In this case, the partial evaluation of Equation (19) involves a reevaluation of the two-body partial derivatives and use of the perturbing acceleration computed in the first evaluation.†† The Predict, Evaluate, Correct, Evaluate (PECE) algorithm was found to be the next most efficient algorithm followed by PE and $PE(CE)^n$. However, for integration of the averaged equations of motion, use of a PECE* algorithm coupled with 11th-order integration formulas unnecessarily limits the integration stepsize. The more stable PECE algorithm is, appropriate for this application when used with integration orders ninth or lower.

This conclusion is demonstrated in Table 11, where results are presented from a calibration of the numerical averaging orbit generator for a 30-day prediction of the AE-C circular orbit (see Table 2).

Errors are listed that were obtained in the radius of perigee, $r_p$, and in the mean longitude, $\lambda$, predictions. The total number of force evaluations required for a 30-day prediction, which is directly proportional to the computational cost, is also listed. This comparison of the PECE* and PECE algorithms demonstrates that the relatively small stepsizes that must be used with the PECE* algorithm severely limit its efficiency. The authors plan to investigate increasing the efficiency of an averaged orbit generator by the use of a modified PECE* algorithm in which the dominant perturbation is reevaluated. It is thought that such an algorithm will exhibit a numerical stability near that of the PECE algorithm at a considerably reduced cost.

In addition, an examination of results in Table 11 that were obtained using a PECE algorithm yields the conclusion that, for large stepsizes, reducing the order of the integrator improves both the resulting accuracy and the efficiency. The improvement in efficiency arises from a reduction in the number of correction iterations required for convergence of the multistep starting procedure.

In the numerical computation of averaged element rates arising from discontinuous perturbations (such as drag and solar radiation pressure), a more accurate evaluation of the averaged element rates can be achieved by evaluating the averaged derivatives only over the interval of nonzero perturbation. In such cases, the equation for the averaged element rates is evaluated as follows:

$$\frac{\overline{da_\alpha(t_o)}}{dt} = \frac{1}{2\pi} \int_{F_o-\pi}^{F_o+\pi} \frac{r}{a} \left[\frac{da_\alpha(F)}{dt}\right]_C dF + \frac{1}{2\pi} \int_{F_1}^{F_2} \frac{r}{a} \left[\frac{da_\alpha(F)}{dt}\right]_D dF + \frac{1}{2\pi} \int_{F_3}^{F_4} \frac{r}{a} \left[\frac{da_\alpha(F)}{dt}\right]_S dF$$

where $F_o$ = value of the eccentric longitude at time $t_o$

$\frac{\overline{da_\alpha}}{dt}$ = averaged orbital element rate

$\left[\frac{da_\alpha}{dt}\right]_C$ = orbital element rate arising from the continuous perturbations

$\left[\frac{da_\alpha}{dt}\right]_D$ = orbital element rate arising from drag

$\left[\frac{da_\alpha}{dt}\right]_S$ = orbital element rate arising from solar radiation pressure

† A Class I differential equation is of the form

$$\dot{y} = f(y, x)$$

†† A recent investigation (Reference 45) has shown that for some satellite orbits a final partial evaluation that includes a reevaluation of the dominant perturbing acceleration is optimal.

$n$ = Kepler mean motion

$a$ = semimajor axis

$r$ = magnitude of the position vector

$F_1$ = value of the eccentric longitude at entrance into the atmosphere

$F_2$ = value of the eccentric longitude at exit from the atmosphere

$F_3$ = value of the eccentric longitude at entry into sunlight

$F_4$ = value of the eccentric longitude at exit from sunlight

The quantities $F_1$ and $F_2$ are determined using two-body mechanics. The quantities $F_3$ and $F_4$ are obtained by solving the shadow equation given in Appendix C. The consequent elimination of irregularities from the derivative history improves the stability of the equations of motion, permitting the use of a larger stepsize.

This effect has been demonstrated for the case of a discontinuity in the drag perturbation. In Tables 12 and 13, results from a calibration of a numerically averaged orbit generator are shown for predictions of the AE-C elliptic orbit (see Table 3) of length 30 and 90 days, respectively. The procedure that averages the effects of the total perturbing acceleration vector in a single quadrature is labeled "single quadrature." The procedure that averages the effects of drag and the effects of the continuous perturbing accelerations in two separate quadrature computations is labeled "two quadratures." An inspection of the accuracies achieved with these two procedures shows that, without special treatment of the drag perturbation, the stepsize is limited to 4 hours. However, when the averaged element rates caused by drag are computed only over the drag perturbed region, stepsizes as large as 2 days yield comparable accuracies.

A comparison of the accuracies achieved in 30-day prediction using various integration orders with the two quadrature process indicates the orders 5 through 9 yield identical results for stepsizes as large as 2 days. However, the efficiency of the lower orders is greater. On the other hand, if the same comparison is made for the 90-day predictions, an order 5 integration process is clearly superior to orders 7 and 9 for use with the 2-day stepsize. This occurrence is an indication of numerical instability in the seventh and higher order integration processes. This instability does not manifest itself in the 30-day predictions due to the small (about 10) number of integration steps involved.

In summary, a suitable integration procedure for the averaged equations of motion combines Adams multistep integration methods (of orders 4 through 7) with a Predict, Evaluate, Correct, Evaluate integration algorithm.

Osculating-to-Mean Element Conversion

The question of the importance of using mean initial values for the orbital elements with an averaged prediction method is the subject of current research. The use of initial osculating elements rather than mean elements results in a phase difference between the mean and osculating orbits that increases much more rapidly with time than if mean elements had been used. For long-term calculations of orbital element histories for which this type of disagreement with the osculating orbit can be tolerated, mean initial elements probably are not needed.[14] However, for applications of averaging methods such as prediction of tracking schedules or orbital lifetimes, the conversion of osculating initial conditions to mean can make the difference between satisfactory and unsatisfactory methods of prediction. In addition, for the statistical determination of mean elements using the averaged equations as a dynamical model, a priori mean elements increase the probability of convergence of a least-squares estimation procedure. Therefore, to take full advantage of the possible applications of an averaged prediction capability, the conversion of osculating to mean elements is required. This section discusses various conversion procedures and presents an evaluation of the resulting mean elements.

The conversion of osculating to mean elements can be handled either analytically or numerically. The best known analytic method is an iterative procedure based on Brouwer theory.[40, 46] This approach is limited by the fact that drag and lunar-solar effects are not included in the conversion. It will be demonstrated below that for strongly drag-perturbed orbits such as the AE-C elliptic orbit (Table 3) or strongly lunar-perturbed orbits such as the IMP type (Tables 5 and 6), this is a significant limitation.

A numerical conversion can be performed using either of the following procedures:

1. Differentially correcting the initial state vector using high-precision observations and an averaged prediction model.

2. Solving the set of integral equations

$$\bar{a}_\alpha(t_0) = \frac{1}{2\pi\bar{T}} \int_{t_0-\bar{T}/2}^{t_0+\bar{T}/2} a_\alpha(t)\,dt \tag{77}$$

where $\bar{a}_\alpha(t_0)$ = mean orbital element at the time of interest

$\bar{T}$ = mean period

$a_\alpha(t)$ = osculating orbital element at time $t$

In both of these procedures, the appropriate length for the averaging interval also deserves consideration.

Musen and Smith[47] used a procedure related to procedure 2 above to compute mean orbital elements for an IMP orbit similar to that given in Table 5 that has a 6-day period. In this regard, they computed the mean period over an interval equal to approximately the lunar period (five satellite revolutions). The mean elements were then computed over one or two mean periods. The authors are investigating the possible advantage of using multirevolution averaging intervals in the conversion process to more exactly average out the effects of medium period oscillations. For example, for the IMP mission orbit (Table 6), which has an orbital period that is in nearly 2:1 resonance with the lunar period, use of a two-revolution averaging interval is being investigated.

The authors have experimented with the above methods to obtain mean elements for several orbit types. Figure 1 presents a comparison of semimajor axis predictions that were obtained using a high-precision, time-regularized orbit generator with predictions obtained using a numerical averaging orbit generator. The test case is the AE-C elliptic orbit (Table 3) perturbed by $J_2$ and $J_3$ harmonic effects, solar and lunar point mass effects and atmospheric drag. Clearly, for this orbit, the use of Brouwer mean elements offers no improvement over the use of osculating initial elements. The mean elements labeled "type 1" were obtained using procedure 1, given above.

The Differential Correction procedure that was used in this conversion consists of a weighted least-squares estimator coupled to a numerically averaged orbit generation process. The partial derivatives of the state vector with respect to the initial state vector are approximated by analytical two-body expressions. The Differential Correction was performed over one revolution of simulated observations, which were computed using a high-precision orbit generator. Figure 1 shows that the prediction obtained using the mean elements computed using the first conversion procedure is clearly superior to that obtained using osculating initial conditions. The divergence of the mean from the osculating prediction after 80 days can arise from small errors in the initial mean orbital elements. The appearance of this discrepancy in a region of rapid semimajor axis decay can also be an indication of a breakdown in the correctness of the averaging assumption of constancy of the slowly varying elements over one orbital period.

An implementation of the second conversion procedure has been suggested previously by Uphoff.[14] He suggests performing a one-revolution precision numerical integration and, at the same time, evaluating Equation (77) for the mean semimajor axis at each integration step. This procedure is terminated when the integration time is equal to the mean period derived from the current value computed for the mean semimajor axis.

The authors are currently implementing conversion procedure 2, above, in the following manner. First, the integral equation for the mean semimajor axis [Equation (77)] is solved iteratively to obtain the mean period. The required values of a (t) are computed from the position and velocity vectors at time t, which are obtained by interpolation from a file of accelerations that were computed using a high-precision orbit generator. This procedure will be available for conversion of input conditions at the beginning of an ephemeris generation or differential correction run, as well as for the conversion of the converged osculating results at the end of a differential correction run.

## Optimization of Averaging Methods

Because the chief advantage of averaging methods is their efficiency, considerable attention has been paid to maximizing this characteristic. This problem can be approached from two directions:

1. Reduction of the cost-per-integration step of evaluating the orbital element rates.
2. Reduction in the total number of integration steps required for computation of a given arc by improving the accuracy and numerical stability of the equations of motion.

This section discusses the application of these techniques to optimization of averaging methods.

In cases for which the averaged derivatives are computed numerically, the cost of a derivative evaluation can often be reduced significantly by choosing the lowest quadrature order that gives the desired accuracy. However, this choice is orbit-dependent.

For example, for predictions of the AE-C circular orbit (Table 2), use of a 12th-order quadrature for computation of the averaged rates yields nearly the same results as use of a 24th-order quadrature. This conclusion is demonstrated in Table 11 for a computation of the numerically averaged rates arising from the total perturbation model. Table 14 presents a comparison of AE-C circular orbit predictions that were made using analytically averaged expressions for the rates arising from $J_2$, $J_3$, solar, and lunar effects and a numerical quadrature technique for computation of the averaged rates arising from atmospheric drag. An examination of these results indicates that among the orders tested, a 12th-order quadrature is probably optimum for computation of the averaged rates arising from atmospheric drag. Results presented in Table 17 for computations of the ESSA-8 orbit (Table 4) using a numerically averaged orbit generator demonstrate that a 12th-order quadrature can be used successfully for this application as well. Similarly, in the numerical computation of the averaged rates caused by lunar effects for the IMP-J orbits, a 9th-order quadrature was found to be sufficient for most applications.[42] This result is demonstrated in Figure 2. Nearly equivalent orbital predictions were obtained with a 9th-order quadrature as with a 24th-order process.

On the other hand, for the AE-C elliptic orbit (Table 3), a 24th-order quadrature was found to be necessary for computation of the averaged rates arising from both atmospheric drag and continuous perturbations. Figure 3 demonstrates this conclusion for computation of the averaged rates arising from atmospheric drag. Figure 3 presents a comparison of semimajor axis predictions for the AE-C elliptic orbit. In these predictions, analytically averaged expressions were used in the computation of the averaged rates arising from the $J_2$, $J_3$, solar, and lunar perturbations. A numerical quadrature was used only in the computation of the perturbing acceleration arising from atmospheric drag. As the order of the quadrature is increased, the predictions approach the solution obtained using the 24th-order solution. A prediction was also made using a 23rd-order quadrature process. The predicted semimajor axis agrees to within 4 kilometers at 90 days with the 24th-order solution. This result indicates that for predictions in this accuracy range, a 24th-order quadrature is necessary.

In addition, it might be possible to reduce the cost-per-integration step by using an analytical model rather than a numerical method for computing the averaged derivatives. Because analytical models usually are based on a set of limiting assumptions, care must be taken that the model is appropriate to the orbit of interest. Good examples of this are NEMD calculations (Tables 1, 9, 10), which were made using a hybrid averaging procedure. The zonal harmonic and the solar effects were computed analytically and the lunar effects were computed either analytically or numerically. For the same stepsize, the ratio of the corresponding computational cost was 1:6. This result indicates that it might be possible to achieve a substantial improvement in the efficiency of an averaged orbit generation process by using the appropriate analytical expressions for the averaged element rates in place of numerical averaging computations. The authors plan to extend their investigation to include comparisons of analytical and numerical averaging computations for oblateness and solar point mass effects within the same program structure.

The following are methods for reducing the total number of integration steps required to achieve a certain accuracy. A reduction in the error that is introduced at each derivative evaluation reduces the resulting global error, permitting the use of larger integration stepsizes. Special treatment of the equations of motion arising from discontinuous perturbations, which was discussed above, is an improvement that falls in this category. In addition, choosing a multirevolution averaging interval to average out the medium period effects of a resonant perturbation more completely might also produce a similar improvement. This smoothing process results in increased numerical stability in the equations of motion. Such a stabilization effect is indicated for computation of lunar effects on the IMP-J mission orbit (see Table 6) for which a near 2:1 resonance exists between the lunar and satellite periods.[42] Results from 3-year predictions that were computed by numerically averaging over one and two revolutions are presented in Tables 15 and 16, respectively. A comparison of these results shows that the latter process yields a slower growth of error with stepsize.

A careful choice of the perturbation model can reduce random errors. For the case of a close-Earth satellite, such as ESSA-8 (Table 4), the inclusion of the tesseral and sectoral harmonics in the 4 x 4 gravitational model used in the integration of the averaged dynamics severely increases the error of the prediction for a given stepsize. This conclusion was derived from the results presented in Table 17. For this orbit, at a stepsize of 2 days, the error in a 14-day semimajor axis prediction increases from 0.0003 kilometer to 0.13 kilometer with the addition of the tesseral and sectoral harmonics. An analysis of this orbit to determine the dominant harmonic terms in the gravitational model shows that the only important tesseral and sectoral terms are of order 13.[48] Therefore, the inclusion of tesseral and sectoral terms in the gravitational model introduces unnecessary errors, rather than improving the solution. This conclusion has been substantiated in Differential Correction (DC) studies performed on ESSA-8 data using a numerically averaged prediction model to obtain mean elements. In this investigation, a DC was performed at one epoch, the converged results were propagated for 14 days, and a second DC was performed at this second epoch. The predicted and converged state vectors were then compared with the corrected osculating state vector. The results of these comparisons, which are given in Table 18, show that smaller residuals and comparable prediction errors in the position vector were obtained using a fourth-order zonal model, compared to results obtained using a full fourth-order gravity model. It is possible to use a stepsize as large as 12 hours with the fourth-order zonal model. Whereas, the prediction errors in Table 17 indicate that this would not be possible with the full fourth-order model. Clearly, the appropriateness of the perturbation model to the satellite orbit of interest should be given careful attention.

## Future Work

At several points this paper, specific problems areas were identified. This paragraph provides a unified discussion of those aspects of the method of averaging that require further consideration.

As indicated in the section entitled Optimization of Averaging Methods, numerical evidence (based on testing of ESMAP for the NEMD case) indicates that analytical averaging can be much more efficient than numerical averaging procedures in terms of computational cost. However, some perturbations (notably atmospheric drag) do not readily admit to an analytical averaging process. Thus, in general, a hybrid averaging method might be optimum in which oblateness and lunar-solar effects are treated analytically and drag is treated via numerical quadrature. As yet the question has not been resolved of whether the same computational advantage remains when an analytically averaged orbit generation process is called by a complicated trajectory program, such as GTDS, which has various interface complexities including ephemeris files, sophisticated triggering options, and comprehensive input and output options. This problem deserves further consideration.

Further development of analytically averaged equations of motion in terms of the equinoctial elements is needed. While the nonsingular variables have definite advantages, many analytical results that are relevant to the method of averaging have been derived only in terms of the classical orbital element formulation. For example, consider the role played by the inclination functions $F_{lmp}(i)$ the Hansen coefficients $X_0^{l,k}$, which are used in the lunar-solar disturbing function and in the gravitational potential. In terms of these functions, the analytically averaged equations of motion for the lunar-solar and gravitational perturbations can be expressed in a very concise form.[15] The analogs of these functions probably exist in nonsingular variables but their derivation represents a comprehensive task in terms of algebraic manipulation. For this application, the use of a computer program for the automated manipulation of literal Poisson series is recommended. R. Broucke, Jet Propulsion Laboratory, has initiated an effort to modify an existing Poisson series manipulation system[49] to work in equinoctial coordinates. At present the Keplerian portion of the system has been modified to treat h and k as polynomial variables and $\lambda$ as a trignometric variable. The following series have been generated: $F - \lambda$, $\sin(F - \lambda)$, $\cos(F - \lambda)$, $\sin F$, $\cos F$, $a/r$, and $r/a$. The completed nonsingular Keplerian processor will have the capability to generate analytically averaged equations of motion.

The disadvantage of the choice of h and k as polynomial variables is that h and k are treated as small parameters. It might be possible to modify the set of nonsingular variables such that the Poisson series processing is exact. One modification of the element set is given in Chapter 5 of Reference 41.

An averaged orbit generation method based on the formulation in Reference 41 deserves consideration from another point of view. Due to the simplified equations of motion, the derivation of the differential equations for the state transition matrix is greatly simplified relative to the derivation of the state transition matrix differential equations for the equinoctial elements.[6]

With respect to applications, a calibration of the first-order averaging process is needed. This calibration should include an evaluation for operational support applications such as network maintenance. The importance of the osculating to mean element transformation for various applications should also be considered, as well as the most efficient choice for the quadrature order when numerical averaging is used. This evaluation should also include a comparison of the numerical error bounds with those attributed to the averaged orbit generation process in References 50 and 51.

Development of second or higher order averaging procedures also deserves attention. For the orbital predictions of strongly drag-perturbed satellites, there is numerical evidence that a breakdown in the first-order averaging assumption might introduce significant errors. Thus, higher order averaging theories might extend the range of applicability of long-term methods of orbit prediction. It is recommended that the development of higher order averaging methods start with the basic averaging expansions presented in the section entitled Averaged Orbit Generation Methods and in Reference 7.

## Concluding Remarks

In this paper, a general overview has been presented of the history and current status of the application of the method of averages to problems in orbit determination. Analytically averaged orbital element rates have been presented for the equinoctial elements for the oblateness and third-body perturbations. A numerical averaging process in terms of equinoctial elements has also been included. For the integration of the averaged equations of motion, low-order multistep integration formulas used in a PECE algorithm are recommended. The importance of careful treatment of discontinuous perturbations and of an osculating to mean element transformation was demonstrated. Methods for optimization of an averaged orbit generation process were indicated, such as a reduction in the quadrature order in numerical averaging and the use of analytical rather than numerical averaging whenever possible. In addition, areas that require further consideration to develop an optimum averaged orbit generation process have been indicated.

The equations of motion of a satellite are expressed by the general formula

$$\ddot{\vec{r}} + \frac{\mu \vec{r}}{|\vec{r}|^3} = \vec{P} \tag{A-1}$$

where $\vec{r}$ = position vector in the inertial Cartesian coordinate system

$\ddot{\vec{r}}$ = acceleration vector in the inertial Cartesian coordinate system

$\mu$ = gravitational constant

$\vec{P}$ = total perturbing acceleration

Solutions to the unperturbed problem

$$\ddot{\vec{x}} + \frac{\mu \vec{x}}{|\vec{x}|^3} = 0 \tag{A-2}$$

can be written as

$$\vec{x} = \vec{x}[\vec{a}(t)] \tag{A-3}$$

$$\dot{\vec{x}} = \frac{\partial \vec{x}}{\partial \vec{a}} \cdot \dot{\vec{a}} \tag{A-4}$$

where $\vec{a}$ is a vector of orbit elements for which the determinant

$$\left| \frac{\partial \vec{a}}{\partial \vec{x}} \,\middle|\, \frac{\partial \vec{a}}{\partial \dot{\vec{x}}} \right| \neq 0 \tag{A-5}$$

where $\frac{\partial \vec{a}}{\partial \vec{x}}$ and $\frac{\partial \vec{a}}{\partial \dot{\vec{x}}}$ are $6 \times 3$ matrices of partial derivatives.

The variation-of-parameters (VOP) method is based on the concept of treating a perturbed satellite orbit as a continually changing conic section or osculating orbit. With this method, solutions $\vec{r}(t)$ are sought to Equation (A-1) of the form Equation (A-3), but having orbit elements that vary with time. Therefore, at any time, t, $\vec{r}$ and $\vec{x}$ can be related as follows:

$$\vec{r}(t) = \vec{x}[\vec{a}(t)] \tag{A-6}$$

The rate of change of the orbital element with respect to the reference motion can be separated out as follows:

$$\dot{\vec{a}} = \dot{\vec{a}}^{(u)} + \dot{\vec{a}}^{(p)} \tag{A-7}$$

where $\dot{\vec{a}}^{(u)}$ *are the element rates for the case* $P = 0$ *and* $\dot{\vec{a}}^{(p)}$ are the element rates arising from the perturbations.

Using these definitions and Equation (A-4)

$$\dot{\vec{r}} = \frac{\partial \vec{x}}{\partial \vec{a}} \cdot \dot{\vec{a}} = \dot{\vec{x}} + \frac{\partial \vec{x}}{\partial \vec{a}} \cdot \dot{\vec{a}}^{(p)} \tag{A-8}$$

$$\begin{aligned} \ddot{\vec{r}} &= \frac{d}{dt}\left(\frac{\partial \vec{x}}{\partial \vec{a}} \cdot \dot{\vec{a}}\right) = \ddot{\vec{x}} + \frac{\partial \dot{\vec{x}}}{\partial \vec{a}} \cdot \dot{\vec{a}}^{(p)} \\ &+ \frac{d}{dt}\left(\frac{\partial \vec{x}}{\partial \vec{a}} \cdot \dot{\vec{a}}^{(p)}\right) \end{aligned} \tag{A-9}$$

where $\frac{\partial \vec{x}}{\partial \vec{a}}$ and $\frac{\partial \dot{\vec{x}}}{\partial \vec{a}}$ are $3 \times 6$ matrices of partial derivatives.

Substituting Equations (A-6) and (A-9) into Equation (A-1) gives three equations involving six variables. To make the problem definite, three additional conditions are chosen. It is advantageous to make the following choice

$$\frac{\partial \vec{x}}{\partial \vec{a}} \cdot \dot{\vec{a}}^{(p)} = 0 \tag{A-10}$$

which matches the formula for the unperturbed velocity to that giving the actual velocity. With this restriction, the velocity in Equation (A-8) reduces to that for unperturbed motion in Equation (A-4). Therefore, the orbit is specified by an instantaneous set of orbit elements. Position and velocity can then be determined from these osculating orbit elements using the formulas of unperturbed elliptic motion.

Substituting Equations (A-6) and (A-9) into Equation (A-1) and imposing the condition given in Equation (A-10) yields

$$\ddot{\vec{x}} + \frac{\partial \dot{\vec{x}}}{\partial \vec{a}} \cdot \dot{\vec{a}}^{(p)} = \vec{P} - \frac{\mu \vec{x}}{|\vec{x}|^3} \tag{A-11}$$

Using the fact that the functions $\vec{x}$ and $\dot{\vec{x}}$ are solutions to the unperturbed problem [Equation (A-2)], Equation (A-11) reduces to

$$\frac{\partial \dot{\vec{x}}}{\partial \vec{a}} \cdot \dot{\vec{a}}^{(p)} = \vec{P} \tag{A-12}$$

This equation, with Equation (A-10), gives the system of equations to be solved

$$\begin{bmatrix} \frac{\partial \dot{\vec{x}}}{\partial \vec{a}} \\ \hline \frac{\partial \vec{x}}{\partial \vec{a}} \end{bmatrix} \dot{\vec{a}}^{(p)} = \begin{bmatrix} \vec{P} \\ \hline 0 \end{bmatrix} \tag{A-13}$$

Using the properties of the two-body matrizant (Reference 12), this set of equations can be solved for $\dot{\vec{a}}^{(p)}$, yielding the VOP equations

$$\dot{\vec{a}}^{(p)} = \left[ \frac{\partial \vec{a}}{\partial \dot{\vec{x}}} \,\middle|\, \frac{\partial a}{\partial \vec{x}} \right] \begin{bmatrix} \vec{P} \\ 0 \end{bmatrix} \tag{A-14}$$

$$\dot{\vec{a}}^{(p)} = \frac{\partial \vec{a}}{\partial \dot{\vec{x}}} \cdot \vec{P} \tag{A-15}$$

The orbital parameters at a specific time are obtained by integrating the equations of motion numerically. These equations can be expressed in a different form by using the fact that a conservative force is equal to the gradient of a potential function. Thus,

$$\vec{P} = \vec{\nabla}R + \vec{Q} \tag{A-16}$$

where R = perturbing potential due to conservative forces

$\vec{Q}$ = perturbing acceleration due to nonconservative forces

Substituting Equation (A-16) into Equation (A-15) gives the set of equations

$$\dot{a}_i^{(p)} = \frac{\partial a_i}{\partial \vec{x}} \cdot \frac{\partial R}{\partial \vec{x}} + \frac{\partial a_i}{\partial \vec{\dot{x}}} \cdot \vec{Q} \tag{A-17}$$

Using the relationship[12]

$$\frac{\partial a_i}{\partial \vec{\dot{x}}} = -\sum_{j=1}^{6} (a_i\,,\,a_j)\,\frac{\partial \vec{x}}{\partial a_j} \tag{A-18}$$

where $(a_i, a_j)$ = Poisson brackets,

yields

$$\dot{a}_i^{(p)} = -\sum_{j=1}^{6} (a_i\,,\,a_j)\,\frac{\partial R}{\partial a_j} + \frac{\partial a_i}{\partial \vec{\dot{x}}} \cdot \vec{Q} \tag{A-19}$$

This form for the VOP equations is useful when the averaged dynamics are under consideration.

## Appendix B - Two-Body Mechanics With Equinoctial Elements

### Transformation from Classical Elements to Equinoctial Elements

The direct equinoctial elements are given by

$$\begin{aligned} a &= a \\ h &= e \sin(\omega + \Omega) \\ k &= e \cos(\omega + \Omega) \\ \lambda_o &= M_o + \omega + \Omega \\ p &= \tan(i/2) \sin\Omega \\ q &= \tan(i/2) \cos\Omega \end{aligned} \tag{B-1}$$

where a, e, i, $M_o$, $\omega$, and $\Omega$ are the classical orbit elements. The elements h and k are the components (in the orbital frame) of the eccentricity vector that points toward the perigee and has the magnitude e. Elements p and q are required in the rotation matrix between the inertial frame and the orbital frame. The element $\lambda_o$ is the mean longitude in the classical literature. The retrograde equinoctial elements are given by

$$\begin{aligned} a &= a \\ h_r &= e \sin(\omega - \Omega) \\ k_r &= e \cos(\omega - \Omega) \\ \lambda_{or} &= M_o + \omega - \Omega \\ p_r &= \cot(i/2) \sin\Omega \\ q_r &= \cot(i/2) \cos\Omega \end{aligned} \tag{B-2}$$

The quantities $h_r$ and $k_r$ are the components of the eccentricity vector relative to the retrograde orbital frame. The elements $p_r$ and $q_r$ are required in the rotation matrix between the inertial frame and the retrograde orbital frame.

The orbital coordinate frames can be defined in terms of the classical orbital elements; this is done in Figure 4 for the direct case and in Figure 5 for the retrograde case. In Figures 4 and 5, unit vector $\hat{w}$ is the normal to the orbit plane. For the direct case the $\hat{f}$ and $\hat{g}$ unit vectors are in the orbital plane. The direction of the $\hat{f}$ unit vector depends on the classical orbit elements $\Omega$ and i. The unit vector $\hat{g}$ completes the right-handed triad of $\hat{f}$, $\hat{g}$, and $\hat{w}$. For the retrograde case, the $\hat{f}^*$, $\hat{g}^*$, and $\hat{w}$ unit vectors comprise the right-handed triad. Mathematically, the unit vectors can be expressed in terms of the equinoctial elements by

$$\hat{f} = \frac{1}{1 + p^2 + q^2} \begin{pmatrix} 1 - p^2 + q^2 \\ 2\,pq \\ -2p\,I \end{pmatrix} \tag{B-3}$$

$$\hat{g} = \frac{1}{1 + p^2 + q^2} \begin{pmatrix} 2\,pq\,I \\ (1 + p^2 - q^2)\,I \\ 2q \end{pmatrix} \tag{B-4}$$

$$\hat{w} = \frac{1}{1 + p^2 + q^2} \begin{pmatrix} 2p \\ -2q \\ (1 - p^2 - q^2)\,I \end{pmatrix} \tag{B-5}$$

Equations (B-3), (B-4), and (B-5) require some comment. If I = +1, the p and q elements defined in Equation (B-1) must be used in Equations (B-3), (B-4), and (B-5). The $\hat{f}$, $\hat{g}$, and $\hat{w}$ unit vectors computed with I = +1 have the meaning indicated in Figure 4. If I = -1, the retrograde p and q defined in Equation (B-2) must be used in Equations (B-3), (B-4), and (B-5). The $\hat{f}$, $\hat{g}$, and $\hat{w}$ unit vectors computed with I = -1 have the meaning indicated in Figure 5. This notation will reduce the repetition of almost identical formulas in the remainder of the paper.

## Transformation from Position and Velocity to Equinoctial Elements

This paragraph gives the formulas required to compute the equinoctial elements from the position and velocity. The semi-major axis is

$$a = \left( \frac{2}{|\vec{x}|} - \frac{|\dot{\vec{x}}|^2}{\mu} \right)^{-1} \tag{B-6}$$

The eccentricity vector is given by

$$\vec{e} = -\frac{\vec{x}}{|\vec{x}|} - \frac{(\vec{x} \times \dot{\vec{x}}) \times \dot{\vec{x}}}{\mu} \tag{B-7}$$

The unit vector normal to the orbital plane is given by

$$\hat{w} = \frac{\vec{x} \times \dot{\vec{x}}}{|\vec{x} \times \dot{\vec{x}}|} \tag{B-8}$$

Unit vector $\hat{w}$ has the exact same meaning in Equation (B-8) as in Equation (B-5). These relationships lead to

$$p = \frac{\hat{w}_x}{1 + \hat{w}_z I} \tag{B-9}$$

$$q = \frac{-\hat{w}_y}{1 + \hat{w}_z I} \tag{B-10}$$

In Equations (B-9) and (B-10), if $I = +1$, the p and q [defined in Equation (B-1)] result. If $I = -1$, the retrograde p and q [defined in Equation (B-2)] result. The unit vectors $\hat{f}$ and $\hat{g}$ (or $\hat{f}^*$ and $\hat{g}^*$) may now be computed using Equations (B-3) and (B-4). The equinoctial orbital elements h and k are computed using the formulas

$$h = \vec{e} \cdot \hat{g} \tag{B-11}$$

$$k = \vec{e} \cdot \hat{f} \tag{B-12}$$

If I was set equal to -1 in Equations (B-3) and (B-4), $\hat{f}^*$ and $\hat{g}^*$ were computed and Equations (B-11) and (B-12) give $h_r$ and $k_r$:

$$h_r = \vec{e} \cdot \hat{g}^* \tag{B-13}$$

$$k_r = \vec{e} \cdot \hat{f}^* \tag{B-14}$$

The only remaining element to be computed is the mean longitude, $\lambda$. We first compute the position coordinates $X_1$ and $Y_1$ relative to the orbital frame $\hat{f}$, $\hat{g}$, $\hat{w}$ by

$$X_1 = \vec{x} \cdot \hat{f} \tag{B-15}$$

$$Y_1 = \vec{x} \cdot \hat{g} \tag{B-16}$$

Then we compute

$$\cos F = k + \frac{(1 - k^2 \beta) X_1 - hk\beta Y_1}{a\sqrt{1 - h^2 - k^2}} \tag{B-17}$$

$$\sin F = h + \frac{(1 - h^2\beta) Y_1 - hk\beta X_1}{a\sqrt{1 - h^2 - k^2}} \tag{B-18}$$

where the auxiliary variable $\beta$ is

$$\beta \equiv \frac{1}{1 + \sqrt{1 - h^2 - k^2}} \tag{B-19}$$

The mean longitude $\lambda$ is given by

$$\lambda = F - k \sin F + h \cos F \tag{B-20}$$

For the retrograde case, the quantities $\hat{f}^*$, $\hat{g}^*$, $h_r$, and $k_r$ should replace $\hat{f}$, $\hat{g}$, h, and k in Equations (B-15) through (B-20). The result of Equation (B-20) is the retrograde mean longitude defined in Equation (B-2). The derivation of Equations (B-17), (B-18), and (B-20) is explained in the next paragraph.

## Transformation from Equinoctial Elements to Position and Velocity

*The key to this formulation is the use of the longitudes* $\lambda$, F, and L, defined by

$$\begin{aligned} \lambda &= M + \omega + \Omega \\ F &= E + \omega + \Omega \\ L &= v + \omega + \Omega \end{aligned} \tag{B-21}$$

where M, E, and v are the classical anomalies. Elementary manipulations show that Kepler's equation can be written in terms of the eccentric longitude F

$$\lambda = F + h \cos F - k \sin F \tag{B-22}$$

Once Kepler's equation has been solved, the position and velocity vectors can be expressed as

$$\vec{x} = X_1 \hat{f} + Y_1 \hat{g} \tag{B-23}$$

and

$$\dot{\vec{x}} = \dot{X}_1 \hat{f} + \dot{Y}_1 \hat{g} \tag{B-24}$$

In these equations the unit vectors $\hat{f}$ and $\hat{g}$ are computed using Equations (B-3) and (B-4). The coordinates $X_1$, $Y_1$, $\dot{X}_1$, and $\dot{Y}_1$ relative to the equinoctial frame are given by

$$X_1 = a\left[(1 - h^2\beta) \cos F + hk\beta \sin F - k\right] \tag{B-25}$$

$$Y_1 = a\left[(1 - k^2\beta) \sin F + hk\beta \cos F - h\right] \tag{B-26}$$

$$\dot{X}_1 = \frac{na^2}{r}\left[hk\beta \cos F - (1 - h^2\beta) \sin F\right] \tag{B-27}$$

$$\dot{Y}_1 = \frac{na^2}{r}\left[(1 - k^2\beta) \cos F - hk\beta \sin F\right] \tag{B-28}$$

where the auxiliary equation

$$\frac{r}{a} = 1 - k \cos F - h \sin F \tag{B-29}$$

is necessary for the velocity coordinates. The coordinates can also be expressed in terms of the true longitude by

$$X_1 = r \cos L \tag{B-30}$$

$$Y_1 = r \sin L \tag{B-31}$$

$$\dot{X}_1 = \frac{-na}{\sqrt{1 - h^2 - k^2}} (h + \sin L) \tag{B-32}$$

$$\dot{Y}_1 = \frac{na}{\sqrt{1 - h^2 - k^2}} (k + \cos L) \tag{B-33}$$

$$r = a(1 - h^2 - k^2)/(1 + k \cos L + h \sin L) \tag{B-34}$$

Equations (B-30) through (B-34) will be used in the numerical averaging procedure for the atmospheric drag. Also, the right-hand side of Equation (B-30) can be set equal to the right-hand side of Equation (B-25). This relation and one involving Equations (B-31) and (B-26) can be solved simultaneously to give Equations (B-17) and (B-18).

For the retrograde case, the longitudes are defined by

$$\begin{aligned} \lambda^* &= M + \omega - \Omega \\ F^* &= E + \omega - \Omega \\ L^* &= v + \omega - \Omega \end{aligned} \tag{B-35}$$

and the quantities $\lambda^*$, $F^*$, $L^*$, $\hat{f}^*$, $\hat{g}^*$, $h_r$, and $k_r$ replace the direct variables in Equations (B-22) through (B-34).

Poisson Brackets

In the present application, the Poisson brackets must be given in terms of the equinoctial elements. The results are obtained by direct substitution into the previous results by Broucke and Cefola[34] and are listed in Table 19.

Partial Derivatives of the Equinoctial Elements With Respect to Velocity

The partial derivatives $\partial a/\partial \dot{\vec{x}}$, $\partial p/\partial \dot{\vec{x}}$, and $\partial q/\partial \dot{\vec{x}}$ are obtained directly as functions of the equinoctial elements by using the results of Broucke and Cefola.[34] However, the expressions for $\partial h/\partial \dot{\vec{x}}$, $\partial k/\partial \dot{\vec{x}}$, and $\partial \lambda_o/\partial \dot{\vec{x}}$ in terms of the classical orbit elements are not so easily translated into the equinoctial elements. To compute these quantities, we have to use the relationship

$$\frac{\partial a_\alpha}{\partial \dot{\vec{x}}} = - \sum_{\beta=1}^{6} (a_\alpha, a_\beta) \frac{\partial \vec{x}}{\partial a_\beta} \tag{B-36}$$

which requires the Poisson brackets from Table 19 and the partial derivatives of the position vector. For $\partial \vec{x}/\partial h$ and $\partial \vec{x}/\partial k$, we need the partial derivatives of $X_1$ and $Y_1$, which are

$$\begin{aligned} \frac{\partial X_1}{\partial h} &= -\frac{k\beta \dot{X}_1}{n} + \frac{a}{G} Y_1 \dot{Y}_1 \\ \frac{\partial X_1}{\partial k} &= \frac{h\beta \dot{X}_1}{n} + \frac{a}{G}(\dot{X}_1 Y_1 - G) \\ \frac{\partial Y_1}{\partial h} &= -\frac{k\beta \dot{Y}_1}{n} - \frac{a}{G}(X_1 \dot{Y}_1 + G) \\ \frac{\partial Y_1}{\partial k} &= -\frac{a}{G} X_1 \dot{X}_1 + \frac{h\beta \dot{Y}_1}{n} \end{aligned} \tag{B-37}$$

With these results, the position partials can be specified, as shown in Table 20. Substitution of the results of Tables 19 and 20 into Equation (B-36) gives the desired results, which are listed in Table 21. Note that the above expressions and those for $\partial h/\partial \dot{\vec{x}}$, $\partial k/\partial \dot{\vec{x}}$, and $\partial \lambda/\partial \dot{\vec{x}}$ in Table 21 are greatly simplified relative to the expressions for the same quantities that were given in Reference 35. This simplification, in turn, simplifies the derivation of the differential equations governing the partial derivatives of the mean elements with respect to mean elements at some fixed epoch. (See Reference 6 for a derivation of the differential equations governing the partial derivatives based on the equinoctial formulation presented in Reference 35.)

Finally, it is possible to express the matrix $\partial a_\alpha/\partial \dot{\vec{x}}$ in a variety of coordinate systems. The expression for $\partial a_\alpha/\partial \dot{\vec{x}}$ in terms of the unit vectors

$$\hat{u}_T = \frac{\dot{\vec{x}}}{|\dot{\vec{x}}|} \tag{B-38}$$

$$\hat{u}_N = \hat{w} \times \frac{\dot{\vec{x}}}{|\dot{\vec{x}}|} \tag{B-39}$$

and $\hat{w}$ is given in Table 22 and has particular application in the computation of drag perturbations via the numerical averaging technique.

In terms of equinoctial variables, the shadow equation[52] for the entry and exit values of the true longitude is given by

$$S = 1 - m^2 (1 + k \cos L + h \sin L)^2 - (\alpha \cos L + \beta \sin L)^2 = 0 \tag{C-1}$$

where $m = \dfrac{r_e}{a\sqrt{1 - h^2 - k^2}}$

$$\alpha = \hat{R}_s \cdot \hat{f}$$

$$\beta = \hat{R}_s \cdot \hat{g}$$

In the above equations, $r_e$ is the mean equatorial radius to the Earth and $\hat{R}_s$ is a unit vector pointing to the Sun. To obtain the solution to Equation (C-1), the following quartic equation must be solved:

$$A_0 \cos^4 L + A_1 \cos^3 L + A_2 \cos^2 L + A_3 \cos L + A_4 = 0 \tag{C-2}$$

where $A_0 = 4B^2 + C^2$

$$A_1 = 8Bm^2h + 4Cm^2k$$

$$A_2 = -4B^2 + 4m^4h^2 - 2DC + 4m^4k^2$$

$$A_3 = -8Bm^2h - 4Dm^2k$$

$$A_4 = -4m^4h^2 + D^2$$

$$B = \alpha\beta + m^2hk$$

$$C = \alpha^2 - \beta^2 + m^2 (k^2 - h^2)$$

$$D = 1 - \beta^2 - m^2 (1 + h^2)$$

*The real-valued solutions to the quartic must be sorted to eliminate extraneous roots and to determine the entry* and exit values of true longitude. In addition, solution of Equation (C-2) determines only the magnitudes of the true longitude that satisfy Equation (C-2). The correct values of the true longitude must satisfy Equation (C-1) as well as the condition

$$\hat{R}_s \cdot \hat{r} = \alpha \cos L + \beta \sin L < 0$$

At entry into shadow, the following condition must hold

$$\frac{\partial S}{\partial L} < 0$$

and, at exit from shadow,

$$\frac{\partial S}{\partial L} > 0$$

Previously, the shadow equation has been formulated in terms of equinoctial variables by Edelbaum[6] using the eccentric longitude as the angular variable. The formulation presented above is considerably simpler.

## REFERENCES


1. Boggs, D., "An Algorithm for Integrating Lifetime Orbits in Multirevolution Steps" (AAS Paper No. 68-142, presented at the AAS/AIAA Astrodynamics Specialist Conference, Jackson, Wyoming, September 1968)

2. Velez, C. E., Numerical Integration of Orbits in Multirevolution Steps, NASA Technical Note D-5915, 1970

3. Graf, O.E., and D. G. Bettis, "Modified Multirevolution Integration Methods for Satellite Orbit Computation" (presented at the AAS/AIAA Astrodynamics Specialist Conference, Vail, Colorado, July 1973)

4. Mace, D., and H. Thomas, "An Extrapolation Formula for Stepping the Calculation of the Orbit of an Artificial Satellite Several Revolutions Ahead at a Time," The Astronomical Journal, vol. 65, no. 5, June 1960, pp. 300-303

5. Cohen, C., and E. Hubbard, "An Algorithm Applicable to Numerical Integration of Orbits in Multirevolution Steps," The Astronomical Journal, vol. 65, no. 8, October 1960, pp. 454-456

6. Edelbaum, T. N., L. L. Sackett, and H. L. Malchow, "Optimal Low-Thrust Geocentric Transfer" (AIAA preprint 73-1074, presented at the AIAA 10th Electric Propulsion Conference, Lake Tahoe, Nevada, October 1973)

7. Nayfeh, A., Perturbation Methods, New York: John Wiley and Sons, 1973

8. Bogoliubov, N., and Y. Mitropolski, Asymptotic Methods in the Theory of Nonlinear Oscillations, New York: Gordon and Breach, 1961

9. Apostal, T., Mathematical Analysis, Reading, Massachusetts: Addison-Wesley, 1957, p. 220

10. Broucke, R., A Note on Velocity-Related Series Expansions in the Two-Body Problem, Jet Propulsion Laboratory, Pasadena, California (copy available from author)

11. Brouwer, D., and G. Clemence, Methods of Celestial Mechanics, New York: Academic Press, 1961

12. Broucke, R., "On the Matrizant of the Two-Body Problem," Astronomy and Astrophysics, 1970, vol. 6, pp. 173-182.

13. Kaufman, B., and R. Dasenbrock, "Semianalytic Theory of Long-Term Behavior of Earth and Lunar Orbiters," Journal of Spacecraft and Rockets, vol. 10, no. 6, June 1973, pp. 377-383

14. Uphoff, C., "Numerical Averaging in Orbit Prediction," AIAA Journal, vol. 11, no. 11, November 1973, pp. 1512-1516

15. Cook, G. E., "Basic Theory for Prod, a Program for Computing the Development of Satellite Orbits," Celestial Mechanics, vol. 7, no. 3, April 1973

16. Roth, E., "Fast Computation of High Eccentricity Orbits by the Stroboscopic Method," Celestial Mechanics, vol. 8, no. 2, September 1973

17. Lorell, J., and A. Liu, Method of Averages Expansions for Artificial Satellite Applications, Jet Propulsion Laboratory, Technical Report 32-1513, April 1971

18. Wagner, C. A., The ROAD Program, Goddard Space Flight Center, January 1973 (copy available from author)

19. Kozai, Y., A New Method to Compute Lunisolar Perturbations in Satellite Motions, Smithsonian Astrophysical Observatory, Special Report 349, February 1973

20. Giacaglia, G. E., Lunar Perturbations on Artificial Satellites of the Earth, Smithsonian Astrophysical Observatory, Special Report 352, October 1973

21. Schubart, J., "Long-Period Effects in the Motion of Hilda-Type Planets," Astronomical Journal, vol. 73, no. 2, part 1, March 1968, pp. 99-103

22. Williams, J. G., "Resonances in the Neptune-Pluto System," Astronomical Journal, vol. 76, no. 2, March 1971, pp. 167-177

23. Lorell, J., "Lunar Orbiter Gravity Analysis," The Moon, 1970, vol. 1, no. 2, pp. 190-231

24. Liu, A., and P. Laing, "Lunar Gravity Analysis From Long-Term Effects," Science, vol. 173, September 10, 1971, pp 1017-1020

25. Ferrari, A. J., "Lunar Gravity Derived From Long-Period Satellite Motion - A Proposed Method," Celestial Mechanics, vol. 7, no. 1, 1973, pp. 46-76

26. Ferrari, A. J., and E. J. Christensen, "Mars Gravity Derived From the Long-Period Motion of Mariner 9," (Presented at AAS/AIAA Astrodynamics Conference, Vail, Colorado, July 1973)

27. Breedlove, W. J., Jr., Determination of the Atmospheric and Gravitational Parameters of Mars From a Study of the Long-Period Motion of a Viking Orbiter, Technical Report, School of Engineering, Old Dominion University, Norfolk, Va., July 1972

28. Lorell, J., et al, "Gravity Field of Mars From Mariner 9 Tracking Data," Icarus, vol. 18, no. 2, February 1973

29. Wagner, C. A., "Zonal Gravity Harmonics From Long Satellite Arcs by a Semi-Numeric Method," JGR, vol. 78, no. 17, pp. 3271-3280, 1973

30. Kaula, W., "Development of the Lunar and Solar Disturbing Functions for a Close Satellite," The Astronomical Journal, vol. 67, no. 5, June 1962

31. King-Hele, D. G., Theory of Satellite Orbits in an Atmosphere, Butterworths, London, 1964

32. Olyanyuk, P. V., L. M. Romanov, and V. I. Mikhailik, "On the Peculiarities of Determining Various Systems of the Orbital Elements of a Spacecraft," Translated from Kosmicheskie Issledovaniva, January - February 1971, vol. 9, no. 1, pp. 49-53

33. Kamel, A., and R. Tibbitts, "Some Useful Results on Initial Node Locations for Near-Equatorial Circular Satellite Orbits," Celestial Mechanics, vol. 8, no. 1, August 1973, pp. 45-73

34. Broucke, R., and P. Cefola, "On the Equinoctial Orbit Elements," Celestial Mechanics, vol. 5, no. 3, pp. 303-310

35. Cefola, P. J., "Equinoctial Orbit Elements - *Application of Artificial Satellite Orbits,*" (presented at the AIAA/AAS Astrodynamics Conference, Palo Alto, California, September 1972)

36. O'Neill, V. J., Comparison of Equinoctial Elements and Brouwer Set III Elements for Differential Orbit Correction, Jet Propulsion Lab Technical Memorandum 391-307, March 27, 1972

37. Cefola, P. J., B. A. Lamers, G. Holloway, Jr., and W. D. McClain, The Long-Term Prediction of Artificial Satellite Orbits, Computer Sciences Corporation, Technical Report 9101-14300-01TR, March 1973

38. Plummer, H. C., An Introductory Treatise on Dynamical Astronomy, New York: Dover Publications, Inc., 1960

39. Lorell, J., and A. Liu, Method of Averages Expansions for Artificial Satellite Applications, Jet Propulsion Laboratory, Technical Report 32-1513, April 1971

40. Brouwer, D., "Artificial Satellite Theory Without Drag," Astronomical Journal, 1959, vol. 64, pp. 378-397

41. Long, A., K. Nimitz, and P. Cefola, The Next Generation of Orbit Prediction Formulations for Artificial Satellites II, Computer Sciences Corporation, 9101-14600-01TR, March 1973

42. Long, A., and G. Holloway, Jr., Numerical Testing of ESMAP for Very Long Period Artificial Satellite Orbits, Computer Sciences Corporation 3000-05200-01TM, October 1973

43. Hull, T. E., et al, "Comparing Numerical Methods for Ordinary Differential Equations," SIAM J. Numerical Analysis, vol. 2, no. 4, 603-637, December 1972

44. Moore, H., "Comparison of Numerical Integration Techniques for Orbital Applications" (presented at SIAM Conference on Numerical Integration of Ordinary Differential Equations, Austin, Texas, October 19, 1972)

45. Velez, C., " Summary of Research Activities," (presented at Astrodynamics and Geodynamics Conference at Goddard Space Flight Center, October 15, 1973)

46. Walter, H. G., "Conversion of Osculating Orbital Elements into Mean Elements," The Astronomical Journal, vol. 72, no. 8, October 1967, pp. 994-997

47. Smith, A. J., Jr., A Discussion of Halphen's Method for Secular Perturbations and Its Application to the Determination of Long Range Effects in the Motions of Celestial Bodies, Part 2, National Aeronautics and Space Administration, TR R-194 June 1964

48. Gideon, G. S., Resonant Satellite Geodesy Study Final Report, TRW Report No. 09128.6001-R000

49. Broucke, R., A Programming System for Analytical Series Expansion on the 360-91 Computer (IBM), University of California at Los Angeles (copy made available by author)

50. Brown, A., and W. Pon, "Same Comments on the Error Analysis for the Method of Averaging," (presented at Astrodynamics and Geodynamics Conference at Goddard Space Flight Center, October 16, 1973)

51. Breakwell, J., and J. Vagners, "On Error Bounds and Initialization in Satellite Orbit Theories," Celestial Mechanics, vol. 2, no. 2, July 1970, pp. 253-264

52. Escobal, P., Methods of Orbit Determination, New York: John Wiley and Sons, Inc., 1965, pp. 152-154

Table 1. NASA-ESRO-Mother-Daughter (NEMD) State Vector, Epoch-October 29, 1977 $14^h\ 0.0^m$, Reference Frame-Mean of 1950.0

| OSCULATING ELEMENTS | | | MEAN ELEMENTS | | |
|---|---|---|---|---|---|
| a = | 70849.14233 | km | a = | 70376.60299 | km |
| e = | 0.890723236 | | e = | 0.89014687 | |
| i = | 29.0203198 | deg | i = | 28.970265 | deg |
| $\Omega$ = | 49.4445 | deg | $\Omega$ = | 49.43415 | deg |
| $\omega$ = | 0.2096777488 | deg | $\omega$ = | 0.230115389 | deg |
| M = | 360.0 | deg | M = | 359.99789 | deg |

Table 2. Atmosphere Explorer-C (AE-C) Circular Orbit State Vector, Epoch-August 21, 1974 $10^h\ 24^m\ 0.0^s$, Reference Frame-True of Date

| MEAN ELEMENTS | | |
|---|---|---|
| a = | 6668.14260557 | km |
| e = | 0.0001 | |
| i = | 67.866991779 | deg |
| $\Omega$ = | 92.4004760159 | deg |
| $\omega$ = | 310.292209633 | deg |
| M = | 55.2316996621 | deg |

Table 3. Atmosphere Explorer-C (AE-C) Elliptic Orbit State Vector, Epoch-February 26, 1974 $10^h\ 24^m\ 0.0^s$, Reference Frame-True of Date

| OSCULATING ELEMENTS | | | MEAN ELEMENTS | | |
|---|---|---|---|---|---|
| a = | 8525.7231 | km | a = | 8520.88766 | km |
| e = | 0.23761691 | | e = | 0.237686657 | |
| i = | 68.072741 | deg | i = | 68.0653491 | deg |
| $\Omega$ = | 91.574936 | deg | $\Omega$ = | 91.56476444 | deg |
| $\omega$ = | 93.761824 | deg | $\omega$ = | 93.8385533 | deg |
| M = | 275.36757 | deg | M = | 275.31288 | deg |

Table 4. ESSA-8 State Vector, Epoch-May 29.0, 1970, Reference Frame-True of Date

| OSCULATING ELEMENTS | | | MEAN ELEMENTS | | |
|---|---|---|---|---|---|
| a = | 7822.834 | km | a = | 7815.381 | km |
| e = | 0.00309 | | e = | 0.00284 | |
| i = | 101.802 | deg | i = | 101.811 | deg |
| $\Omega$ = | 207.841 | deg | $\Omega$ = | 207.841 | deg |
| $\omega$ = | 352.742 | deg | $\omega$ = | 348.250 | deg |
| M = | 18.813 | deg | M = | 23.286 | deg |

Table 5. Test Case: Interplanetary Monitoring Platform (IMP) Transfer Orbit State Vector, Epoch-November 1.0, 1973, Reference Frame-Mean of 1950.0

| OSCULATING ELEMENTS | | MEAN ELEMENTS | |
|---|---|---|---|
| a = | 138572.57 | a = | 138592.254 |
| e = | 0.95 | e = | 0.950094 |
| i = | 33.83 | i = | 34.30168 |
| $\Omega$ = | 221.55 | $\Omega$ = | 220.6324 |
| $\omega$ = | 135.73 | $\omega$ = | 136.46 |
| M = | 0.02 | M = | 0.02023 |

Table 6. IMP Mission Orbit State Vector, Epoch-November 1.0, 1973 (Osculating), November 7.0, 1973 (Mean), Reference-Mean of 1950.0

| OSCULATING ELEMENTS | | | MEAN ELEMENTS | | |
|---|---|---|---|---|---|
| a = | 235986.0 | km | a = | 236136.8 | km |
| e = | 0.01 | | e = | 0.04815321 | |
| i = | 32.0 | deg | i = | 32.196 | deg |
| $\Omega$ = | 0.0 | deg | $\Omega$ = | 359.756 | deg |
| $\omega$ = | 30.0 | deg | $\omega$ = | 66.114 | deg |
| M = | 0.0 | deg | M = | 315.739 | deg |

Table 7. General Purpose Averaging Programs in Classical Elements

| PROGRAM | REFERENCE | PERTURBATIONS TREATED VIA ANALYTICAL AVERAGING | PERTURBATIONS TREATED VIA NUMERICAL AVERAGING | COMMENTS |
|---|---|---|---|---|
| KAUFMAN | 13 | LOW-ORDER ZONAL GRAVITY HARMONICS, THIRD BODY | ATMOSPHERIC DRAG; TESSERALS | THIRD-BODY POTENTIAL EXPANDED TO $(a/R_3)^8$; NONROTATING ATMOSPHERE |
| UPHOFF | 14 | | OBLATENESS; DRAG; THIRD-BODY EFFECTS | INCLUDES MODIFICATION FOR CIRCULAR ORBITS |
| COOK | 15 | ZONAL GRAVITY HARMONICS; THIRD BODY | | |
| ROTH | 16 | $J_2$; THIRD BODY | | ALSO INCLUDES TREATMENT OF ATMOSPHERIC DRAG TAKEN FROM *KING-HELE*(31) |
| LORELL | 17 | ZONALS; TESSERALS, THIRD-BODY | | TREATMENT OF TESSERALS ASSUMES THAT CENTRAL BODY ROTATING ANGLE IS FIXED FOR ONE ORBIT OF SATELLITE |
| WAGNER | 18 | ZONALS, THIRD BODY | ATMOSPHERIC DRAG | ANALYTICAL RESULTS FROM KAULA(30) |

Table 8. Auxiliary Parameters for the Third-Body Potential

| | |
|---|---|
| $A_1 = \frac{3}{2} S_2 - 1$ | $B_1 = \frac{3}{2} V_2 + 1$ |
| $A_2 = -\alpha_1 S_4$ | $B_2 = k V_4$ |
| $A_3 = \beta_1 S_5$ | $B_3 = h V_5$ |
| $A_4 = \frac{5}{4} S_2 - 1$ | $B_4 = \frac{3}{4} V_2 - 1$ |
| $A_5 = 105 S_2^2 - 120 S_2 + 24$ | $B_5 = \frac{15}{8} V_2^2 + 5 V_2 + 1$ |
| $A_6 = S_3^2 - 4 S_1^2$ | $B_6 = V_3^2 - 4 V_1^2$ |
| $A_7 = S_1 S_3$ | $B_7 = V_1 V_3$ |
| $A_8 = 7 S_2 - 6$ | $B_8 = V_2 + 2$ |
| $A_9 = \alpha_1 \left(S_3^2 - S_6\right)$ | $B_9 = k \left(V_3^2 - V_6\right)$ |
| $A_{10} = \beta_1 \left(S_3^2 - S_7\right)$ | $B_{10} = h \left(V_3^2 - V_7\right)$ |
| $A_{11} = \alpha_1 \left(S_3^2 - \frac{8}{9} S_4 - 4 \beta_1^4\right)$ | $B_{11} = k V_4 (3 V_2 + 8)$ |
| $A_{12} = \beta_1 \left(S_3^2 - \frac{8}{9} S_5 - 4 \alpha_1^4\right)$ | $B_{12} = h V_5 (3 V_2 + 8)$ |
| $A_{13} = S_2^2 - \frac{4}{3} S_2 + \frac{8}{21}$ | $B_{13} = \frac{5}{8} V_2^2 + \frac{5}{2} V_2 + 1$ |
| $A_{14} = 231 S_2^3 - 378 S_2^2 + 168 S_2 - 16$ | $B_{14} = 35 V_2^3 + 210 V_2^2 + 168 V_2 + 16$ |
| $A_{15} = S_3 \left(S_3^2 - 12 S_1^2\right)$ | $B_{15} = V_3 \left(V_3^2 - 12 V_1^2\right)$ |
| $A_{16} = S_1 \left(3 S_3^2 - 4 S_1^2\right)$ | $B_{16} = V_1 \left(3 V_3^2 - 4 V_1^2\right)$ |
| $A_{17} = A_6 \left(S_2 - \frac{10}{11}\right)$ | $B_{17} = B_6 \left(V_2 + \frac{10}{3}\right)$ |
| $A_{18} = A_7 \left(S_2 - \frac{10}{11}\right)$ | $B_{18} = B_7 \left(V_2 + \frac{10}{3}\right)$ |
| $A_{19} = S_3 \left(S_2^2 - \frac{16}{11} S_2 + \frac{16}{33}\right)$ | $B_{19} = V_3 \left(\frac{5}{16} V_2^2 + \frac{5}{3} V_2 + 1\right)$ |
| $A_{20} = S_1 \left(S_2^2 - \frac{16}{11} S_2 + \frac{16}{33}\right)$ | $B_{20} = V_1 \left(\frac{5}{16} V_2^2 + \frac{5}{3} V_2 + 1\right)$ |

Table 9. $r_p$-Deviation Between Analytical Theory and Numerical Averaging (km)

| TIME FROM EPOCH (DAYS) | $(a/R_3)^2$ | $(a/R_3)^3$ | $(a/R_3)^4$ | $(a/R_3)^5$ |
|---|---|---|---|---|
| 0 | 0.0 | 0.0 | 0.0 | 0.0 |
| 100 | 52.1 | 37.2 | 3.3 | 1.4 |
| 200 | 90.3 | 75.7 | 12.5 | 6.4 |
| 300 | 138.6 | 106.7 | 27.1 | 13.6 |

Table 10. Inclination-Deviation Between Analytical Theory and Numerical Averaging (Degrees)

| TIME FROM EPOCH (DAYS) | $(a/R_3)^2$ | $(a/R_3)^3$ | $(a/R_3)^4$ | $(a/R_3)^5$ |
|---|---|---|---|---|
| 0 | 0.0 | 0.0 | 0.0 | 0.0 |
| 100 | .49 | .43 | .17 | .14 |
| 200 | .64 | .59 | .14 | .11 |
| 300 | .79 | .70 | .13 | .09 |

Table 11. Accuracy and Cost Statistics for 30 Day Predictions of the AE-C Circular Orbit
Perturbation Model: Numerical Averaging-$J_2$, $J_3$, Solar and Lunar Point Masses
Atmospheric Drag (Harris-Priester Model)

| INTEGRATION ALGORITHM | INTEGRATION ORDER | QUADRATURE ORDER | STEPSIZE (HR) | TOTAL FORCE EVALUATIONS | $\Delta r_p$ (KM) | $\Delta\lambda$ (DEG) |
|---|---|---|---|---|---|---|
| PECE | 11 | 24 | 2 | 18000 | REFERENCE | |
| PECE | 11 | 12 | 2 | 9000 | .0003 | .002 |
| PECE | 11 | 12 | 48 | 1570 | .004 | .013 |
| PECE | 9 | 12 | 48 | 1330 | .0007 | .009 |
| PECE | 11 | 12 | 96 | 1880 | .023 | .04 |
| PECE | 9 | 12 | 96 | 1525 | .004 | .013 |
| PECE | 7 | 12 | 96 | 1000 | .001 | .013 |
| PECE* | 7 | 12 | 2 | UNSTABLE | | |
| PECE* | 5 | 12 | 4 | 2500 | .0003 | .001 |
| PECE* | 5 | 12 | 8 | UNSTABLE | | |

Table 12. Accuracy and Cost Statistics for 30 Day Predictions of the AE-C Elliptic Orbit
Perturbation Model: Numerical Averaging-$J_2$, $J_3$, Solar and Lunar Point Masses,
Atmospheric Drag (US '62 Model)

| METHOD | INTEGRATION ALGORITHM | INTEGRATION ORDER | QUADRATURE ORDER | STEPSIZE (HR) | TOTAL FORCE EVALUATIONS | $\lvert\Delta a\rvert$ (km) | $\lvert\Delta r_p\rvert$ (km) |
|---|---|---|---|---|---|---|---|
| SINGLE QUADRATURE | PECE | 9 | 24 | 2 | 18000 | 3.4 | .011 |
| SINGLE QUADRATURE | PECE | 9 | 24 | 8 | 6500 | 14.3 | .056 |
| SINGLE QUADRATURE | PECE | 9 | 24 | 12 | UNSTABLE | | |
| SINGLE QUADRATURE | PECE | 7 | 24 | 12 | UNSTABLE | | |
| TWO QUADRATURES | PECE | 9 | 24 | 2 | 17700 | REFERENCE | |
| TWO QUADRATURES | PECE | 9 | 24 | 8 | 5680 | .002 | .0001 |
| TWO QUADRATURES | PECE | 9 | 24 | 12 | 4200 | .012 | .0002 |
| TWO QUADRATURES | PECE | 7 | 24 | 12 | 3800 | .012 | .0006 |
| TWO QUADRATURES | PECE | 7 | 24 | 24 | 2780 | .052 | .0044 |
| TWO QUADRATURES | PECE | 5 | 24 | 24 | 2250 | .052 | .0048 |
| TWO QUADRATURES | PECE | 9 | 24 | 48 | 3200 | .068 | .006 |
| TWO QUADRATURES | PECE | 7 | 24 | 48 | 2400 | .083 | .008 |
| TWO QUADRATURES | PECE | 5 | 24 | 48 | 1800 | .083 | .009 |

Table 13. Accuracy and Cost Statistics for 90-Day Predictions of the AE-C Elliptic Orbit
Perturbation Model: Numerical Averaging-$J_2$, $J_3$, Solar and Lunar Point Masses,
Atmospheric Drag (US '62 Model)

| METHOD | INTEGRATION ALGORITHM | INTEGRATION ORDER | QUADRATURE ORDER | STEPSIZE (HR) | TOTAL FORCE EVALUATIONS | $\lvert\Delta a\rvert$ (km) | $\lvert\Delta r_p\rvert$ (km) |
|---|---|---|---|---|---|---|---|
| SINGLE QUADRATURE | PECE | 9 | 24 | 2 | 54400 | 7.7 | .37 |
| SINGLE QUADRATURE | PECE | 9 | 24 | 8 | 15480 | 450.0 | 100.0 |
| SINGLE QUADRATURE | PECE | 9 | 24 | 12 | UNSTABLE | | |
| SINGLE QUADRATURE | PECE | 7 | 24 | 12 | UNSTABLE | | |
| TWO QUADRATURES | PECE | 9 | 24 | 2 | 53700 | REFERENCE | |
| TWO QUADRATURES | PECE | 9 | 24 | 8 | 14680 | .28 | .013 |
| TWO QUADRATURES | PECE | 9 | 24 | 12 | 10020 | .55 | .042 |
| TWO QUADRATURES | PECE | 7 | 24 | 12 | 9800 | .55 | .044 |
| TWO QUADRATURES | PECE | 7 | 24 | 24 | 5780 | 3.16 | .06 |
| TWO QUADRATURES | PECE | 5 | 24 | 24 | 5250 | 3.04 | .053 |
| TWO QUADRATURES | PECE | 9 | 24 | 48 | 4600 | 73.0 | 4.1 |
| TWO QUADRATRUES | PECE | 7 | 24 | 48 | 3800 | 5.3 | .11 |
| TWO QUADRATURES | PECE | 5 | 24 | 48 | 3240 | 3.3 | .08 |

Table 14. Comparison of 40 Day Predictions of the AE-C Circular Orbit

Perturbation Model: Analytical Averaging-$J_2$, $J_3$, Sun, Moon
Numerical Averaging-Atmospheric Drag (US '62 Model)

| STEPSIZE (HR) | QUADRATURE ORDER | $\lvert\Delta a\rvert$ (km) | $\lvert\Delta r_p\rvert$ (km) | $\lvert\Delta M\rvert$ (deg) |
|---|---|---|---|---|
| 6 | 24 | REFERENCE | | |
| 24 | 16 | .0003 | .0002 | .01 |
| 24 | 12 | .0003 | .0001 | .001 |
| 24 | 9 | .005 | .006 | .022 |
| 48 | 12 | .003 | .004 | .008 |
| 96 | 12 | .025 | .032 | .38 |

Table 15. Accuracy Statistics for 3-Year Predictions of the IMP Mission Orbit

Perturbation Model: Numerical Averaging-Lunar Point Mass

| STEPSIZE (DAYS) | QUAD-RATURE ORDER | AVERAGING INTERVAL ($2\pi$) | CPU 360/91 (SEC) | $\lvert\Delta a\rvert$ ($10^3$ KM) | $\lvert\Delta e\rvert$ | $\lvert\Delta i\rvert$ (DEG) | $\lvert\Delta\Omega\rvert$ (DEG) | $\lvert\Delta\omega\rvert$ (DEG) | $\lvert\Delta M\rvert$ (DEG) | $\lvert\Delta r_p\rvert$ ($10^3$ KM) |
|---|---|---|---|---|---|---|---|---|---|---|
| .5 | 24 | 1 | REFERENCE | | | | | | | |
| 1 | 24 | 1 | 83 | 0.001 | 0.0002 | – | 0.01 | 0.30 | 1.07 | – |
| 1 | 16 | 1 | 57 | 0.006 | 0.0009 | – | 0.04 | 1.24 | 4.18 | 0.2 |
| 1 | 12 | 1 | 43 | 0.001 | 0.0001 | – | – | 0.26 | 0.97 | – |
| 1 | 9 | 1 | 33 | 0.006 | 0.0015 | 0.02 | 0.08 | 1.99 | 6.5 | 0.4 |
| 2 | 24 | 1 | 42 | 0.125 | 0.0096 | 0.05 | 0.52 | 15.2 | 48.6 | 2.2 |
| 2 | 16 | 1 | 27 | 0.143 | 0.0098 | 0.05 | 0.54 | 15.8 | 50.8 | 2.3 |
| 2 | 12 | 1 | 22 | 0.081 | 0.0088 | 0.05 | 0.45 | 13.8 | 44.2 | 2.0 |
| 2 | 9 | 1 | 18 | 0.005 | 0.0092 | 0.01 | 0.43 | 10.7 | 33.8 | 2.1 |

Table 16. Accuracy Statistics for 3-Year Predictions of the IMP Mission Orbit

Perturbation Model: Numerical Averaging-Lunar Point Mass

| STEPSIZE (DAYS) | QUAD-RATURE ORDER | AVERAGING INTERVAL ($2\pi$) | 360/91 (SEC) | $\lvert\Delta a\rvert$ ($10^3$ KM) | $\lvert\Delta e\rvert$ | $\lvert\Delta i\rvert$ (DEG) | $\lvert\Delta\Omega\rvert$ (DEG) | $\lvert\Delta\omega\rvert$ (DEG) | $\lvert\Delta M\rvert$ (DEG) | $\lvert\Delta r_p\rvert$ ($10^3$ KM) |
|---|---|---|---|---|---|---|---|---|---|---|
| .5 | 24 | 2 | REFERENCE | | | | | | | |
| 1 | 24 | 2 | 82 | 0.001 | 0.0001 | – | 0.01 | 0.15 | 0.5 | – |
| 1 | 12 | 2 | 42 | 0.014 | 0.0003 | – | 0.02 | 0.48 | 1.5 | 0.1 |
| 1 | 9 | 2 | 32 | 0.25 | 0.0035 | 0.02 | 0.59 | 15.6 | 49.0 | 0.8 |
| 2 | 24 | 2 | 41 | 0.53 | 0.001 | 0.01 | 0.04 | 0.95 | 2.9 | 0.1 |
| 2 | 16 | 2 | 29 | 0.319 | 0.003 | 0.02 | 0.07 | 2.4 | 5.1 | 0.4 |
| 2 | 12 | 2 | 22 | 0.233 | 0.0035 | 0.04 | 0.21 | 8.0 | 26.5 | 0.6 |

Table 17. Accuracy and Cost Statistics for 14 Day Predictions of the ESSA-8 Orbit

I. Perturbation Model: Numerical Averaging-4 × 4 Gravity Model, Solar and Lunar Point Masses

| INTEGRATION ALGORITHM | INTEGRATION ORDER | QUADRATURE ORDER | STEP-SIZE (HR) | TOTAL NUMBER OF FORCE EVALUATIONS | $\Delta a$ (KM) | $\Delta\lambda = \Delta M + \Delta\Omega + \Delta\omega$ (DEGREES) |
|---|---|---|---|---|---|---|
| PECE | 11 | 24 | 2 | 12100 | REFERENCE | |
| PECE | 9 | 24 | 2 | 9000 | .007 | .002 |
| PECE | 9 | 12 | 2 | 4500 | .007 | 002 |
| PECE | 9 | 12 | 8 | 1620 | .06 | 2.0 |
| PECE | 9 | 12 | 24 | 1250 | .06 | 5.0 |
| PECE | 7 | 12 | 24 | 950 | .11 | 4.75 |
| PECE | 9 | 12 | 48 | UNSTABLE | | |
| PECE | 5 | 12 | 48 | 775 | .13 | 5.9 |
| PECE* | 7 | 12 | 2 | 2436 | .03 | .02 |
| PECE* | 5 | 12 | 4 | 1296 | .027 | .63 |

II. Perturbation Model: Numerical Averaging- 4 × 0 Gravity Model, Solar and Lunar Point Masses

| INTEGRATION ALGORITHM | INTEGRATION ORDER | QUADRATURE ORDER | STEP-SIZE (HR) | TOTAL NUMBER OF FORCE EVALUATIONS | $\Delta a$ (KM) | $\Delta\lambda$ (DEGREES) |
|---|---|---|---|---|---|---|
| PECE | 9 | 12 | 2 | 5220 | REFERENCE | |
| PECE | 11 | 12 | 24 | UNSTABLE | | |
| PECE | 9 | 12 | 24 | 1020 | .0005 | .005 |
| PECE | 7 | 12 | 48 | UNSTABLE | | |
| PECE | 5 | 12 | 48 | 475 | .0003 | .003 |

Table 18. Comparison of ESSA-8 State Vectors at 14 Days From Epoch

| METHOD | GRAVITY MODEL | STEPSIZE (SEC) | ITERA-TIONS | RMS | X (KM) | Y (KM) | Z (KM) | $\lvert\Delta\vec{r}\rvert$ (KM) |
|---|---|---|---|---|---|---|---|---|
| HIGH PRECISION PREDICTION | 4 X 4 | 60 | | | -395.2772 | -2431.583 | -7402.4749 | 1.4 |
| HIGH PRECISION DC | 4 X 4 | 60 | 10 | .475 | -396.2007 | -2432.6012 | -7402.0741 | REFERENCE |
| AVERAGED PREDICTION | 4 X 4 | 7200 | | | -395.1799 | -2430.8783 | -7400.3624 | 2.58 |
| AVERAGED DC | 4 X 4 | 7200 | 4 | 2.76 | -395.1442 | -2430.4700 | -7400.0408 | 3.17 |
| AVERAGED PREDICTION | 4 X 0 | 7200 | | | -394.8476 | -2430.6275 | -7400.2605 | 3.03 |
| AVERAGED DC | 4 X 0 | 7200 | 4 | 2.02 | -396.6927 | -2431.7530 | -7399.7796 | 2.51 |
| AVERAGED PREDICTION | 4 X 0 | 43200 | | | -394.7206 | -2430.5253 | -7400.3014 | 3.08 |
| AVERAGED DC | 4 X 0 | 43200 | 4 | 2.02 | -396.6929 | -2431.7053 | -7399.7797 | 2.52 |

Table 19. Poisson Brackets of Equinoctial Elements*, **

| | |
|---|---|
| $(a, \lambda_o) = -2a\, s_1$ | $(h, p) = -kp\, s_5$ |
| $(\lambda_o, h) = -h\, s_4$ | $(h, q) = -kq\, s_5$ |
| $(\lambda_o, k) = -k\, s_4$ | $(k, p) = hp\, s_5$ |
| $(\lambda_o, p) = -p\, s_5$ | $(k, q) = hq\, s_5$ |
| $(\lambda_o, q) = -q\, s_5$ | $(p, q) = -\frac{1}{2}\, s_2\, s_5\, I$ |
| $(h, k) = -s_1\, s_3$ | |

*Auxiliary variables:

$$s_1 = 1/na^2$$

$$s_2 = 1 + p^2 + q^2$$

$$s_3 = \sqrt{1 - h^2 - k^2}$$

$$s_4 = s_1\, s_3 / (1 + s_3)$$

$$s_5 = s_1\, s_2 / (2 s_3)$$

**Note: If $I = +1$, the elements have the meaning of Equation (B-1). If $I = -1$, the elements have the meaning of Equation (B-2).

Table 20. Partial Derivatives of Position

$$\frac{\partial \vec{x}}{\partial a} = \frac{1}{a}\left(\vec{x} - \frac{3}{2}\, \dot{\vec{x}}\, t\right)$$

$$\frac{\partial \vec{x}}{\partial h} = \frac{\partial X_1}{\partial h}\, \hat{f} + \frac{\partial Y_1}{\partial h}\, \hat{g}$$

$$\frac{\partial \vec{x}}{\partial k} = \frac{\partial X_1}{\partial k}\, \hat{f} + \frac{\partial Y_1}{\partial k}\, \hat{g}$$

$$\frac{\partial \vec{x}}{\partial \lambda_o} = \dot{\vec{x}} / n$$

$$\frac{\partial \vec{x}}{\partial p} = \frac{2}{1 + p^2 + q^2}\left[q\,(Y_1 \hat{f} - X_1 \hat{g})\, I - X_1 \hat{w}\right]$$

$$\frac{\partial \vec{x}}{\partial q} = \frac{2}{1 + p^2 + q^2}\left[p\,(X_1 \hat{g} - Y_1 \hat{f}) + Y_1 \hat{w}\right] I$$

Table 21. Partial Derivatives of the Equinoctial Elements With Respect to Velocity

$$\frac{\partial a}{\partial \dot{\vec{x}}} = \frac{2 \dot{\vec{x}}}{n^2 a}$$

$$\frac{\partial h}{\partial \dot{\vec{x}}} = -\frac{1}{\mu}\left[G \hat{f} + r \dot{X}_1 \hat{y}\right] + \frac{k}{G}\,(q Y_1 I - p X_1)\, \hat{w}$$

$$\frac{\partial k}{\partial \dot{\vec{x}}} = \frac{1}{\mu}\left[G \hat{g} + r \dot{Y}_1 \hat{y}\right] - \frac{h}{G}\,(q Y_1 I - p X_1)\, \hat{w}$$

$$\frac{\partial p}{\partial \dot{\vec{x}}} = \frac{(1 + p^2 + q^2)\, Y_1 \hat{w}}{2G}$$

$$\frac{\partial q}{\partial \dot{\vec{x}}} = \frac{(1 + p^2 + q^2)\, X_1 \hat{w}}{2G}\, I$$

$$\frac{\partial \lambda}{\partial \dot{\vec{x}}} = \frac{-2}{na^2}\, \vec{r} + \beta\left(k \frac{\partial h}{\partial \dot{\vec{x}}} - h \frac{\partial k}{\partial \dot{\vec{x}}}\right) + \frac{1}{na^2}\,(q I Y_1 - p X_1)\, \hat{w}$$

$$\hat{y} = (\hat{w} \times \vec{x})/r$$

$$G = na^2 \sqrt{1 - h^2 - k^2}$$

Table 22. Partial Derivatives of Equinoctial Elements With Respect to Velocity in Tangential Coordinates

$$\frac{\partial a}{\partial \dot{\vec{x}}} = \frac{2 |\dot{\vec{x}}|}{n^2 a}\, \hat{u}_T$$

$$\frac{\partial h}{\partial \dot{\vec{x}}} = -\frac{2 \dot{X}_1 G}{|\dot{\vec{x}}| \mu}\, \hat{u}_T + \frac{1}{|\dot{\vec{x}}|}\left[\frac{\dot{Y}_1 G}{\mu} - \frac{\dot{X}_1}{G}\,(k Y_1 - h X_1)\right] \hat{u}_N + \frac{(I q Y_1 - p X_1) k}{G}\, \hat{w}$$

$$\frac{\partial k}{\partial \dot{\vec{x}}} = \frac{2 \dot{Y}_1 G}{|\dot{\vec{x}}| \mu}\, \hat{u}_T + \frac{1}{|\dot{\vec{x}}|}\left[\frac{\dot{Y}_1}{G}\,(k Y_1 - h X_1) + \frac{\dot{X}_1 G}{\mu}\right] \hat{u}_N - \frac{(I q Y_1 - p X_1) h}{G}\, \hat{w}$$

$$\frac{\partial p}{\partial \dot{\vec{x}}} = \frac{1 + p^2 + q^2}{2G}\, Y_1 \hat{w}$$

$$\frac{\partial q}{\partial \dot{\vec{x}}} = \frac{(1 + p^2 + q^2) I}{2G}\, X_1 \hat{w}$$

$$\frac{\partial \lambda}{\partial \dot{\vec{x}}} = \frac{2}{|\dot{\vec{x}}|}\left(\frac{na}{G} - \frac{\beta}{r}\right)(h X_1 - k Y_1)\, \hat{u}_T + \frac{1}{|\dot{\vec{x}}|}\left[2 - \frac{\beta r}{a} + \beta (1 - h^2 - k^2)\right] \hat{u}_N + \frac{(I q Y_1 - p X_1)}{G}\, \hat{w}$$

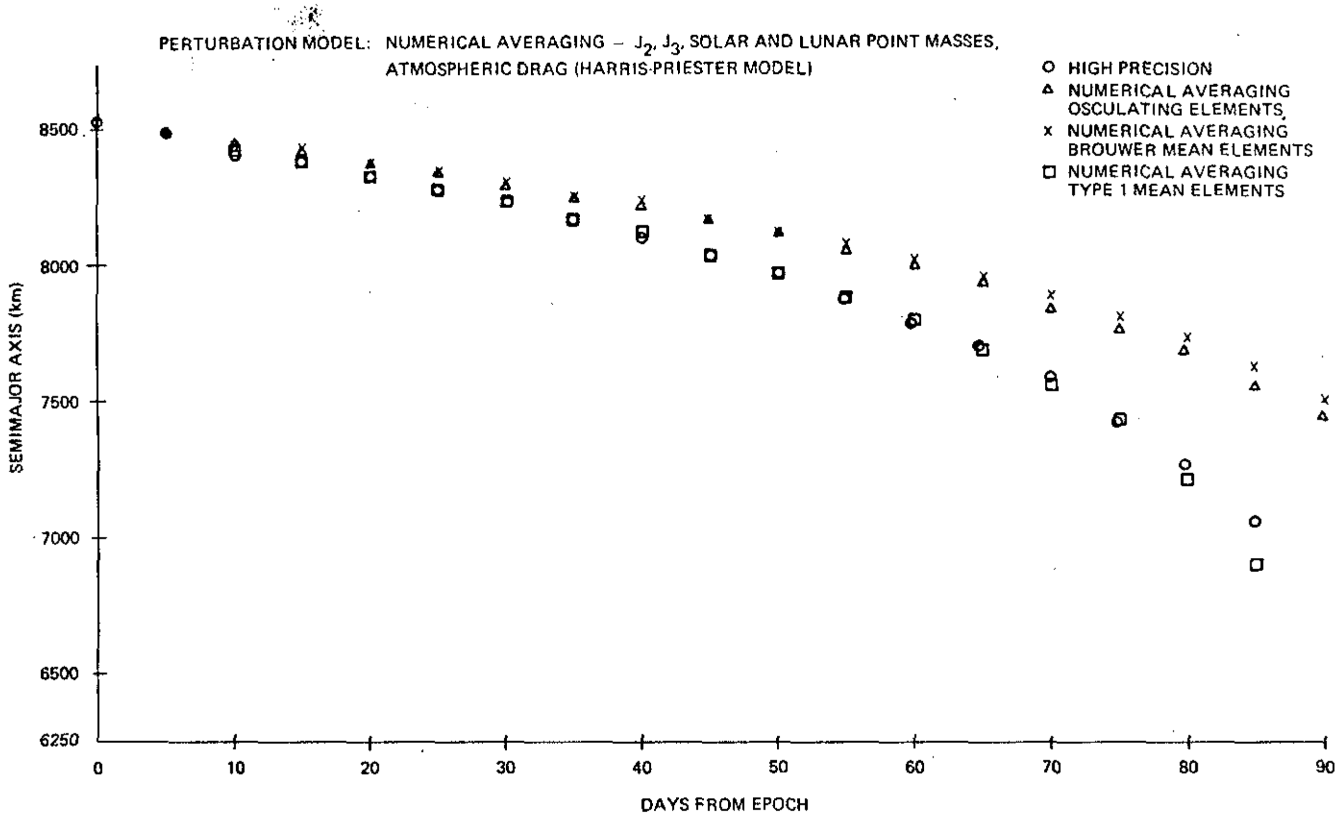


Figure 1. Semimajor Axis Predictions for the AE-C Elliptic Orbit

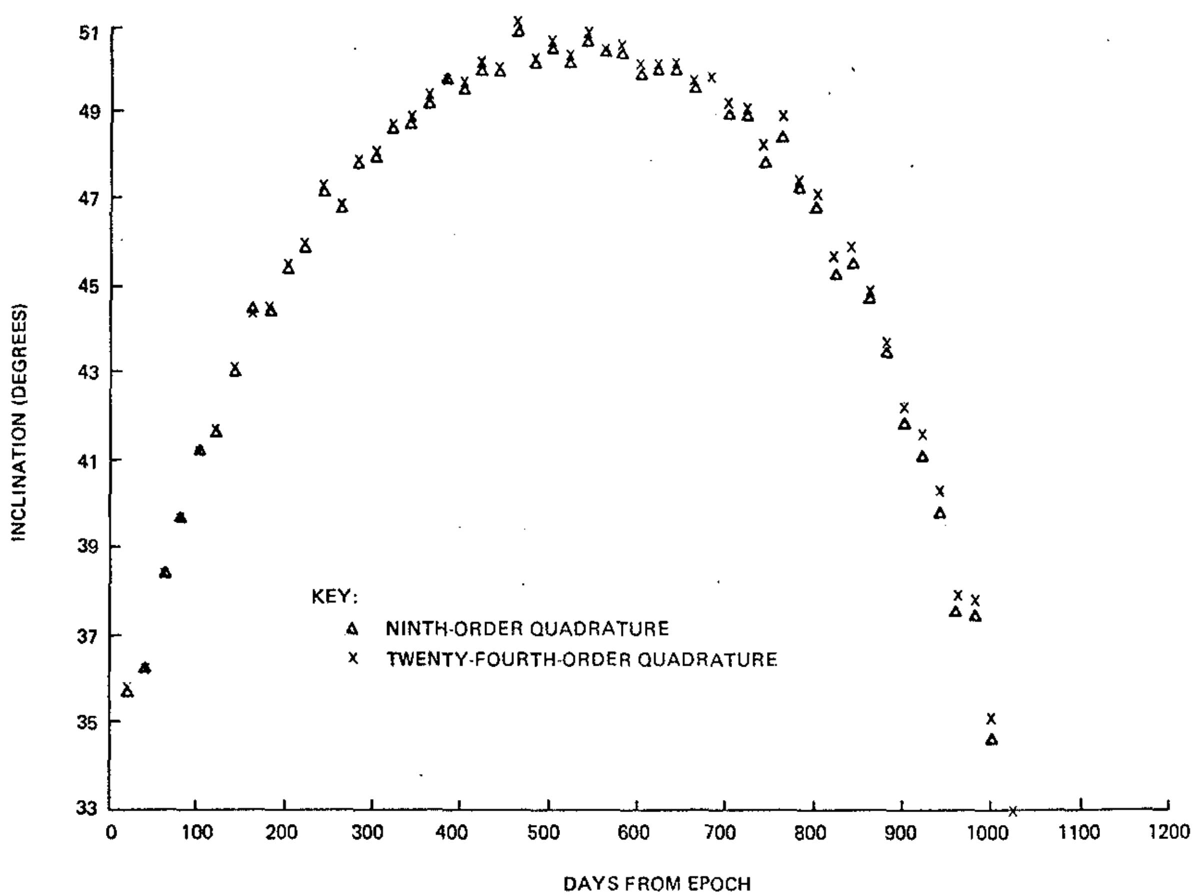


Figure 2. Comparison of Inclination Histories for the IMP-J Transfer Orbit
Perturbation Model: Numerical Averaging-Lunar Point Mass

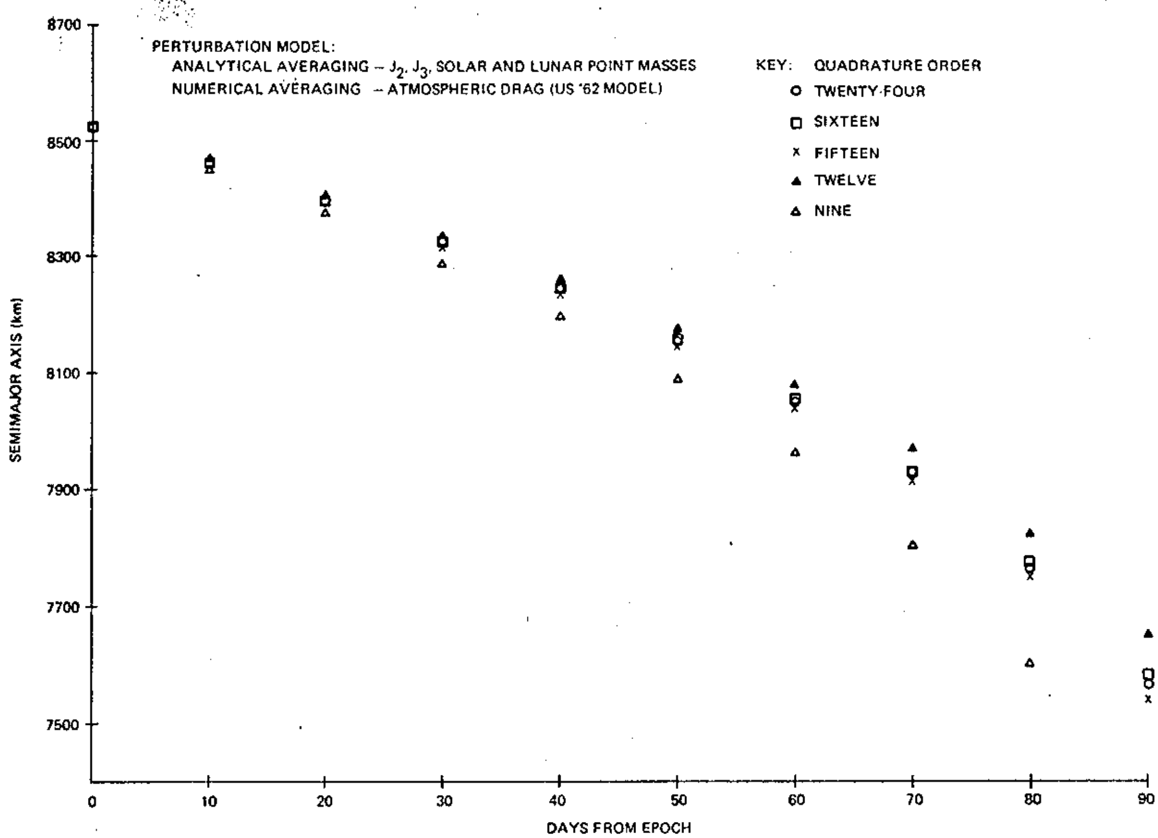


Figure 3. Comparison of Semimajor Predictions for the AE-C Elliptic Orbit Using Various Quadrature Orders

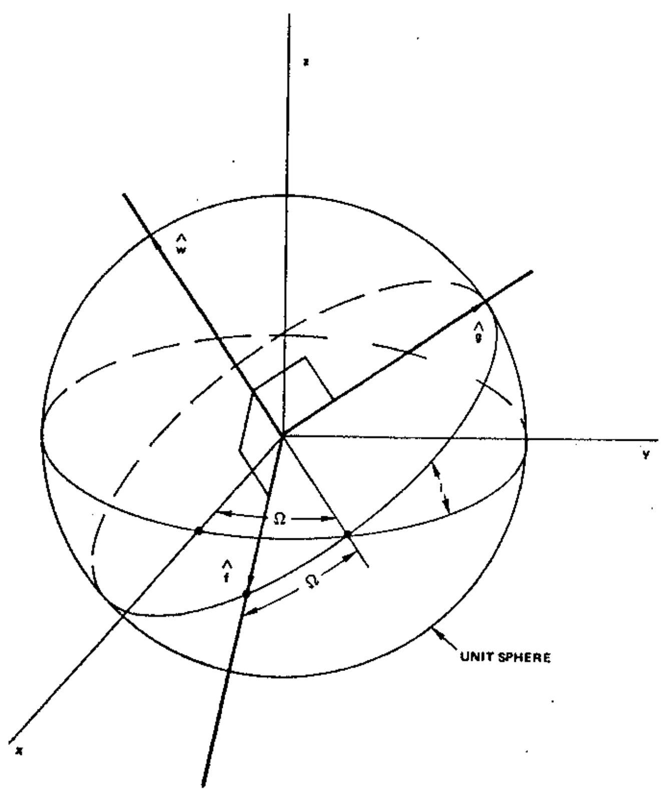


Figure 4. Equinoctial Coordinate Frame

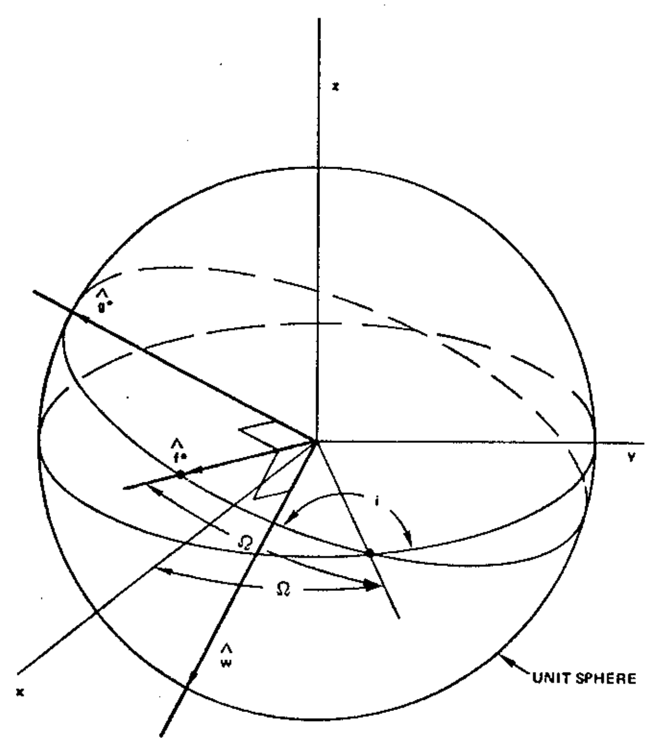


Figure 5. Retrograde Equinoctial Coordinate Frame